Review Article

Mudassir Ur Rahman*, Mohamed Farouk Elsadek*, Rangaswamy Roopashree and Aditya Kashyap

Advancing hydrogen storage and exploring the potential of perovskite hydrides and metal hydrides

https://doi.org/10.1515/revic-2025-0006
Received January 30, 20; accepted May 26, 2025;
published online June 18, 2025

Abstract: Recent notable developments concerning the hydrogen storage materials are summarized in this review, with particular emphasis placed on magnesium hydrides, titanium- and calcium-based hydrides, metal borohydrides, and perovskite-type hydrides. MgH_2 performance is greatly improved through nanostructuring and transition metal doping. Calcium hydrides, as well as titanium hydrides have very good hydrogen storage properties in addition to the potential for superconductivity. Single and bimetallic borohydrides have high hydrogen contents, achieving high performance in battery and energy application, but face challenges in regeneration and stability. Many perovskite-type hydrides, including MgX_3H_8 (X = Sc, Ti, Zr), Li_2CaH_4, and Li_2SrH_4, as well as oxide-based hydrides like $MgTiO_3Hx$, $CaTiO_3Hx$, and $BaYO_3H_x$, are emerging as ideal hydrogen storage materials thanks to their stable crystal structure, promising thermodynamics, excellent mechanical properties, and efficient hydrogen cycling. Destabilization of the hydrogen is likely based on analysis of DFT studies of hydrogen binding enthalpy, which supports stability and negative formation enthalpies for MgX_3H_8 and $BaYO_3H_3$ as well as $CaTiO_3H_6$ and storage of 4.27 wt% with desorption at ~821.1 K further strengthens the potential of perovskite hydrides in a variety of hydrogen storage applications.

Keywords: perovskites; MgH_2; metal borohydrides; alanates; TiH_2; CaH_2

***Corresponding authors: Mudassir Ur Rahman**, Department of Chemistry, GDC Lund Khwar, Abdul Wali Khan University, Mardan, Pakistan, E-mail: mudassir.urrahman262@gmail.com. https://orcid.org/0009-0004-7243-6740 (M.U. Rahman); and **Mohamed Farook Elsadek**, Department of Biochemistry, College of Sciences, King Saud University, Riyadh, Saudi Arabia, E-mail: mfbadr@ksu.edu.sa
Rangaswamy Roopashree, Department of Chemistry, JAIN (Deemed to be University), Bangalore, Karnataka, India
Aditya Kashyap, Center for Research Impact & Outcome, Chitkara University, Rajpura, 140401, Punjab, India

1 Introduction

The global demand for the energy has seen a significant rise in recent years, driven by various factors such as the increasing population, advancements in industrialization, and improvements in living standards. Fossil fuels such as oil, natural gas, etc., have been essential sources of energy for several decades to meet the growing energy demands. The dependence on these non-renewable energy sources highlights the pressing challenges of balancing energy consumption with environmental sustainability and exploring alternative solutions.[1–4] Fossil fuels are currently the primary energy source despite their environmental drawbacks as a polluting option. This reliance stems from the modern lifestyle, characterized by rapid urbanization, population growth and industrial advancements.[5] Globally, the consumption of fossil fuels is projected to increase by nearly 56 % by 2040. However, these energy sources will eventually fall short of meeting the world's growing energy demands. According to the latest statistics, the planet's oil reserves are estimated to last only 41 years. Furthermore, greenhouse gases such as CO_2 are altering global temperatures and triggering various environmental changes.[6] Investigating and developing renewable energy solutions including wind, tidal, Solar, geothermal and other are therefore wise. As compare to fossil fuels, these renewable sources are abundant globally and emit far less carbon dioxide. However, there are drawbacks to their adoption and use, including decreased efficiency, safety issues, and specific environmental effects.[7–9] Nowadays Today, hydrogen has become a key driver in the transformation of global energy technologies, serving as a crucial carrier for low-carbon energy transformation.[10–12] Hydrogen is an excellent alternative to conventional fuels, offering a non-polluting and sustainable energy solution. As a clean, abundant, and renewable fuel, hydrogen releases only water vapor when it is used, making it a clean and low-emission energy source.[13] Apart from its use in transportation, hydrogen can be applied to diverse areas, including stationary systems and portable technologies.[14,15] Conventional fuels like gasoline have an energy

density that is three times lower than hydrogen by weight. These characteristics highlight hydrogen potential as an attractive option for various energy storage systems and as a versatile energy carrier.[16] The challenge of large-scale hydrogen storage after production has become a critical issue to address, as hydrogen releases a high potential yield per unit mass but has a lower energy density per unit volume.[17–19] Approximately 75 % of the observable universe's mass is composed of H-atoms, making it the most abundant element in the cosmos. However, on Earth's surface, hydrogen ranks as the third most abundant element.[20] H_2 isn't naturally found on Earth and can't be directly extracted from water. It needs to be made using energy from hydrogen-rich materials. This makes hydrogen an energy carrier, not a primary fuel source.[21] According to G. A. Olah et al. in The *Methanol Economy (2006)*, approximately 50 million tonnes of hydrogen were produced annually worldwide at that time.[22] Recent IEA's *Hydrogen Breakthrough Agenda Report* data show that approximately 97 million tonnes of hydrogen were produced globally in 2023.[23] The ability to effectively store hydrogen is a critical component for establishing its uses as a primary fuel in transport infrastructure, and it is one of the major applications within the hydrogen-based economy. For hydrogen to become a viable alternative to conventional fuels, advancements in storage technology are essential. These include methods for safely, efficiently, and compactly storing hydrogen at low costs, whether in compressed form, liquid form or solid form. This will enable its widespread adoption in vehicles and other transportation systems, paving the way for a sustainable energy transition.[24] On of the effective and standout approaches in hydrogen storage technologies is solid hydrogen storage. In this process, the hydrogen is inserted into materials such as metal hydrides, chemical hydrides, or absorbents for future use. This technique allows for high-density storage, making it safer and more reliable compared to gaseous or liquid hydrogen forms. Incorporating hydrogen into a stable solid structure reduces risks such as leakage or flammability, enhancing its appeal for various applications, including transportation and energy systems. In this review, we discussed the storage of hydrogen in solid-state form, focusing on new types of solid hydrogen storage materials. Furthermore, various materials classes, including binary hydrides, alanates, borohydrides and perovskite hydrides, are explored for their unique properties and storage mechanisms. Each category offers distinct advantages, such as high hydrogen density and reversible storage capabilities, while facing challenges like thermal stability and kinetics. Through an analysis of emerging research, this review underscores the potential of these materials to drive sustainable energy solutions and identifies future directions for optimizing their performance. The main objective of this review is to store hydrogen in solid-state material. The paper discusses the composition and structure of these materials, looking into their constitution and the factors determining their stability. Key aspects such as hydrogen storage capacity, reversibility, thermodynamics, and kinetics of this entire process are also analyzed.

2 Metal hydrides

Metal-hydrides are attracting a lot of attention because of their potential utilization in various technologies and the curiosity they generate within the scientific community.[25,26] Firstly, metal hydrides are highly regarded as efficient carriers of hydrogen, which is widely recognized as one of the most potential energy sources for the future. Moreover, certain metal hydrides, like PdH_4, have demonstrated intriguing superconducting properties.[27] Metal hydrides are widely recognized for their exceptional capacity to store hydrogen by absorbing it into their structure. The stored hydrogen can be released when needed, either under normal ambient conditions or by applying heat to the storage tank. This unique property enables metal hydrides to function as efficient and reliable materials for hydrogen storage and release, contributing significantly to advancements in clean energy technologies.[6,28–31]

Generally, metal hydrides (MH_x) are formed by reacting metals (M) with hydrogen gas (H_2) under specific temperature and pressure conditions. Diagrammatically, this process can be illustrated as shown in Figure 1:

The general procedure of hydride formation and hydrogen release can be understood by the following reversible reaction:

$$M + \frac{x}{2} H_2 \leftrightharpoons MHx$$

Hydrogen released from metal hydrides, whether as molecules (H_2) or atoms (H), is widely used across various fields. It acts as a clean energy source in fuel cells, powering vehicles and electronics. In industry, it's crucial for making chemicals like ammonia and methanol, and is also used in oil refining. According to Ramachandran et al., hydrogen (H_2) is widely used in industries for producing petrochemicals such as methanol, activating metal catalysts, and as a reducing agent in metallurgical heat treatments. It plays a key role in ammonia synthesis for fertilizers, consuming about 50 % of global hydrogen, and is also used in electronics for silicon processing. Due to its clean-burning nature, hydrogen is

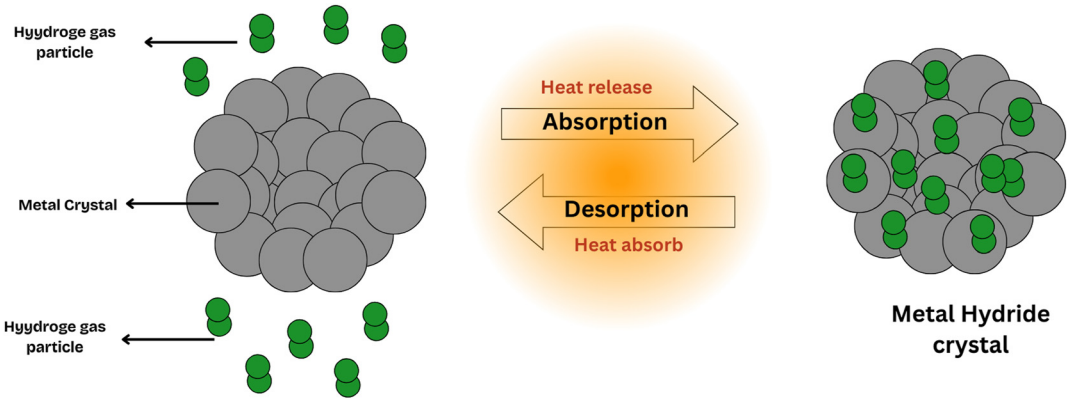

Figure 1: Schematic representation of metal hydride formation. The grey color represents the metal crystal, while the green color indicates the hydrogen molecules.

applied in the flame polishing of glass and optical fiber manufacturing, with growing use in synthetic gas mixtures replacing older systems like dissociated ammonia.[32,33]

2.1 Single metal hydrides

Single metal with hydrogen atoms forms a diverse class of materials with intriguing chemical and physical characteristics. These hydrides are classified based on the type of bonding (Ionic, Covalent, or metallic) between hydrogen atoms and the single metal atom. Both group I and II elements of the periodic table typically form ionic hydrides, where the metal atoms donate electrons to hydrogen atoms and form H^- ions. Transition metals often form covalent hydrides through shared electron pairs between the metal and hydrogen. Metallic hydrides, associated with lanthanides and actinides, exhibit a unique metallic bond and remarkable hydrogen absorption capabilities. These compounds are highly valued for their versatile applications, including efficient hydrogen storage, catalytic processes, and the fabrication of advanced materials, because these materials readily absorb and release hydrogen repeatedly. Nonetheless, challenges such as thermal instability, slow hydrogen absorption/desorption kinetics, and sensitivity to air and moisture continue to inspire ongoing research and innovation in this field.

2.1.1 Magnesium hydrides

Since the beginning of the 21st century, magnesium-based materials have attracted significant interest in the field of hydrogen storage in the solid state due to their plentiful availability, outstanding cycle stability, and eco-friendliness. Compared to other metals, magnesium-based materials stand out for their affordability, large reserves, and superior hydrogen storage capacity, making them especially noteworthy.[34–36]

Magnesium hydrides (MgH_2) stand out as an efficient hydrogen storage material due to their low weight. Wide availability, good chemical properties, and affordability. They offer a high hydrogen density, both gravimetrically and volumetrically, with values of 7.6 wt% and 110 kg H_2m^{-3}, respectively.[37,38] Wagemans et al. found that reducing MgH_2 crystalline size below 1.3 nm decreases stability and enthalpy, with 0.9 nm-sized MgH_2 also storing 10–15 % extra hydrogen on the surface, desorbing at lower temperatures, ideal for PEM fuel cells.[39] Preparing Mg/MgH_2 nanoparticles experimentally is challenging because of the strong reactivity nature of magnesium. Using an electrochemical technique, Aguen Zinsou and colleagues effectively produced surfactant-stability of magnesium nanoparticles with an average diameter of 5 nm in 2008, demonstrating remarkable capability to store hydrogen in solid form. Furthermore, they reported the first instance of hydrogen desorption near room temperature, where nearly complete hydrogen release occurred from colloidal MgH_2 at a low temperature of 85 °C.[40] Lately, the researchers Zhang et al. used a liquid-solid metathesis method powered by ultrasound to create non-confined micro MgH_2 nanoscale particle from 4 nm to 5 nm. At 30 °C, the resultant nanoparticle showed a 6.7 wt percent reversible hydrogen storage capability.[41] Recently, in 2023, Wan and colleagues enhanced the hydrogen storage performance of MgH_2 by doping it with 5 wt% of a high-entropy metallic alloy composed of transitional metals such as Fe, Co, Ni, Cr, and Mn. This alloy significantly reduced the dehydrogenation activation energy from 151.9 to 92.2 kJ/mol and promoted the formation of compounds such as Mg_2Co/Mg_2CoH_5 and Mg_2Ni/Mg_2NiH_4, which facilitated the dehydrogenation process. Remarkably, the composite released 5.6 wt% H_2 within 10 min

at 280 Celsius temperature and absorbed 5.5 wt% H_2 in only 30 s at 150 Celsius temperature.[42] Furthermore, for future performance, doping MgH_2 with various transition metals, such as Fe, Co, Ni, Cr, and Mn, significantly enhances its hydrogen storage performance. These metal dopants serve as effective catalysts, enhancing both the thermodynamic stability and kinetic behavior of hydrogen absorption and release in MgH_2. For example, in another research, Wan et al.[43] studied that doping MgH_2 with Fe significantly improves its hydrogen storage capability. The incorporation of Fe causes lattice distortion and charge transfer, destabilizing MgH_2 and lowering the dehydrogenation activation energy by 44.5 %. This leads to 200 °C reduction in the initial dehydrogenation temperature, and the MgH_2–Fe composite can release 4.5 wt% H_2 at 230 °C within 30 min, making it more efficient materials for hydrogen storage. See Figure 2 for general representation. Zeng et al.[44] stated that Ni doping in Mg/MgH_2 via Ni@rGO nanocomposite improves hydrogen storage properties by lowering hydrogenation/dehydrogenation temperatures (323/479 K) and reducing activation energy (47.0/99.3 kJ mol^{-1}). The composite demonstrates enhanced hydrogen desorption capacity, releasing 1.47 wt% at 498 K within 120 min and 4.30 wt% at 523 K in 30 min, owing to the catalytic effect of Ni.[44] With improved cycling stability and lower operating costs, these improvements may result in faster and more energy-efficient hydrogen storage systems in the future, increasing MgH_2's potential for usage in clean energy technologies like fuel cells and hydrogen-powered cars.

2.1.2 Titanium *hydrides*

Titanium is a valuable metal for cutting-edge industries like aerospace, healthcare and energy production, thanks to its superior resistance to corrosion, high strength to weight ratio and biological compatibility.[45] Titanium hydride (TiH_2) is a chemical compound consisting of titanium and hydrogen, characterized by its grey to black powder form and a face-centred cubic (FCC) crystal structure. It is commonly synthesized by exposing titanium metal to hydrogen gas at elevated temperatures or using plasma-based methods. TiH_2 plays a key role in industries like aerospace, catalysis, and powder metallurgy and is notable for its ability to store hydrogen reversibility. Additionally, it is utilized as a foaming agent in creating metal foams and in pyrotechnics for its reactivity properties. Despite challenges such as reactivity with oxygen and water and thermal instability, TiH_2 is a vital material in energy storage and the development of advanced technologies due to its high efficiency and diverse functionality.[46,47] Recently, numerous studies have focused on developing cost-effective methods for directly producing titanium powder, and the hydrogen-assisted magnesiothermic reduction[48] method is well-known among them and other excellent method is direct reduction of titanium slag.[49] In 2021 Mohammad Rezaei Ardani et al., [50] examined the potential for synthesizing TiH_2 powder by reaction $TiCl_4$ gas with MgH_2 powder. The $TiCl_4$ gas with MgH_2 powder. The $TiCl_4$ gas, derived from the chlorination of nitrided ilmenite, interact with MgH_2 in a hydrogen environment at low temperatures. This method seeks to create an efficient and cost-effective pathway for TiH_2 production, utilizing the chemical interactions between titanium tetrachloride and magnesium hydride under specific conditions. In 2019 I.O. Leipunsky et al., synthesized stoichiometric TiH_2 nanocrystalline powder with a mean particle size of less than 30 nm by utilizing a well-known method of Guen-Miller Flow Levitation. Some well-known methodologies like X-ray photoelectron spectroscopy, HRTEM and X-ray and electron diffraction were utilized to analyze the produced nanopowder, confirming its high quality and nanoscale structure. Hydrogen recovery studies revealed that hydrogen release begins at 390C and peaks at 460C, significantly reducing energy demand compared to commercial-grade TiH_2. This lower thermal requirement highlights the nanopowders efficiency for hydrogen storage and recovery. The research demonstrates that the Guen-Miller FL method reliable produces high-performance stoichiometric TiH_2 nanopowder, maximizing hydrogen content and offering superior characteristics for energy-efficient hydrogen storage and recovery applications.[51]

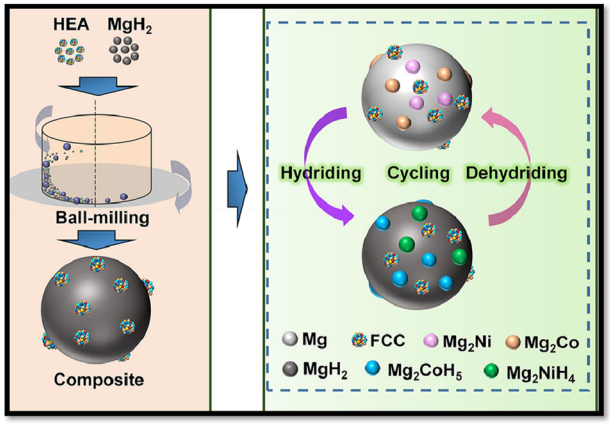

Figure 2: General representation of doping of MgH_2 with transition metals.[42]

2.1.3 Calcium hydrides and clathrate compounds (CaH_2 and CaH_6)

Calcium hydride (CaH_2) is another type of binary metal hydride and grey colour powder, it reacts vigorously with

water, releasing hydrogen gas as a result. This characteristic makes it an effective desiccant[52] or moisture-removing agent.

To investigate the Compton and electronic characteristics of calcium dihydride (CaH_2), Chuan-Yun Xiao et al., used an embedded cluster model and discrete variational local-density functional (DV-LDF) approach. These calculations provide insights into the materials' ionic bonding characteristics, effectively explaining experimental data from photoelectron spectroscopy and Compton profile measurements. Xian's work suggests that doping CaH_2 with a monovalent element might enable superconductivity.[53] The elastic properties of both ionic compounds and partially compounds are commonly evaluated utilizing traditional methods that rely on semi-empirical formulas derived from the Born model.[54] This approach employs central force potentials to represent the ground-state energy of solids based on the arrangement of atomic nuclei. It relies on empirical parameters that define the potentials functional form. These parameters are usually obtained by matching experimental data, such as bond energies, lattice structures, and dielectric properties. The outstanding method such as Hrtree-Fock which is used in crystal, allows ab initio calculation of these properties without relying on experimental data, even for material lacking such information.[55,56] Furthermore, the Hartree–Fock (HF) method, widely recognized for its precision, has proven effective in closely matching experimental elastic constants for both ionic and semi-ionic materials. The electronic and structural characteristics of the CaH_2 crystal, including its band structure, binding energy, elastic constant, and lattice parameters, were examined by Abderrahman et al., utilizing the well-known Hartree-fock ab initio approach. The examination of distribution of charge, states density and band structure offer valuable information about chemical bonding, revealing significant deviations from purely ionic behavior ($Z \approx 1.867$). The elastic constant ($C_{11} = 14.4$, $C_{12} = 110.3$, $C_{13} = 67.9$, $C_{22} = 75.1$, $C_{23} = 143.1$, $C_{33} = 36.6$, $C_{44} = 111.1$, $C_{55} = 68.7$, $C_{66} = 81.6$) and bulk modulus (202.8 GPa) were reported.[57]

Liang Ma et al. (2022), demonstrate that CaH_6, clathrate metal hydride, could be synthesized under extreme conditions, displaying a critical temperature for superconductivity of 215 K at 172 Gpa. This groundbreaking discovery places calcium-based hydrides in a new category of high-temperature superconductors, opening the door to a broader range of hydride materials with unique physical properties.[58] Hui Wang et al. explored CaH_6 at pressure above 150 GPa revealing a unique body-centred cubic structure with hydrogen forming "sodalite" cages that enclose calcium. In this structure, the Ca atom donates electrons to two H_2 units, forming H_4 units that act as building blocks. The electron donation leads to a dynamic Jahn-Teller effect, enhancing electron-phonon coupling and driving superconductivity in CaH_6. The calculated superconducting critical temperature (T_x) of 220–235 K at 150 GPa is the highest all known hydrides.[59] Ying Sun et al. (2024) studied a theoretical overview of hydrogen-rich clathrate super-hydrides, highlighting CaH_6 superconducting potential and its place among the most promising high-temperature superconductors, with an emphasis on the pursuit of room-temperature superconductivity.[60] Decheng An et al. 2024, combine experimental and theoretical analysis, revealing the synthesis of multiple Ca–H phases, including Ca_8H_{46} and exploring how hydrogen vacancies affect superconducting properties. Their work revises the Ca–H phase diagram and links vacancies to changes in critical temperature.[61] Ma Liang et al. 2021, on the other hand, focus on the successful synthesis of CaH_6, reporting its superconducting critical temperature of 215 K at 172 GPa and larger upper critical magnetic field, positioning CaH_6 as an exceptional clathrate hydride among high-T_x superconductors.[62]

2.2 Metal borohydride materials

These are compounds consisting of only one metal (like Li, Na, and K) combine with borohydride ions $[BH_4]^-$. These substances are well-known for high hydrogen storage molecules because they contain a significant amount of hydrogen by weight.

Theoretically, lithium borohydride $LiBH_4$ has an 18.5 % gravimetric hydrogen density, while sodium borohydride $NaBH_4$ has 10.7 %.[63] In metal borohydrides, the bonds between boron and hydrogen are covalent. However, when these ions bond with metals in solid form, the bonding can range from ionic to more covalent, influencing the compound's properties.[64] Lithium boro-hydride ($LiBH_4$) is an important reducing agents and a potential hydrogen storage material.[65] $LiBH_4$ was initially made by reacting lithium ethyl (LiC_2H_5) with diborane (B_2H_6) in toluene solution.[66] Recently, a more direct method using gas-solid reactions has become common. Cai et al., successfully produced $LiBH_4$ reacting a boron source, such as SiB_4/FeB_4/TiB_2, with LiF/LiH in a hydrogen atmosphere. Notably, the SiB_4–LiH–H_2 system can create $LiBH_4$ under relatively mild condition of 250 °C and 10 MPa of hydrogen pressure.[67] A new approach for regenerating $NaBH_4$ was introduced, utilizing real hydrolytic byproducts ($NaBO_2{\cdot}2H_2O$ and $NaBO_2{\cdot}4H_2O$) rather than anhydrous sodium derivatives ($NaBO_2$) to react with magnesium at room temperature and normal atmospheric condition. Furthermore, $NaBH_4$ has been regenerating by

reacting magnesium with $NaBO_2$ (in a water-based solution) and CO_2 using ball milling.[68,69] Figure 4 depicts the $NaBH_4$ crystal structure.[70] The regeneration of $LiBH_4$ from its hydrolysis byproducts has been shown to be achievable with the addition of magnesium through ball milling under normal conditions.[71] $LiBH_4$ usually creates a tetrahedral form (*Pnma* with orthorhombic symmetry and lattice constants of a = 7.17858 Å, b = 4.43686 Å, and c = 6.08321 Å). The crystal structure of $LiBH_4$ changes depending on temperature and pressure. When the temperature exceeds 118 °C, $LiBH_4$ changes from a low-temperature orthorhombic phase (*Pnma*) to a high-temperature hexagonal phase ($P6_3mc$).[72] LiBH4 started to melt at temperatures between 268 and 286 °C. $LiBH_4$ released around 2 wt % of hydrogen during this melting process. At 380 °C temperature NBH_4 begins to release a considerable amount of Hydrogen.[73]

$LiBH_4$ possesses the capacity to store a significant amount of hydrogen, with a theoretical hydrogen storage density of up to 18.5 wt percent. However, only 13.8 wt% of hydrogen is released at 1 bar H_2 and between 380 and 680 degrees Celsius under practical hydrogen release conditions.[74] Other borohydrides, such as Calcium borohydride, were prepared by ball milled $LiBH_4$ and $CaCl_2$, producing LiCl as a byproduct and avoiding reversibility by Nakamori et al.[75] It was more convenient to create calcium borohydrides by reacting Calcium hydrides (CaH_2) with Magnesium bromide (MgB_2) at 400 degrees Celsius with 350 bar of H_2 pressure, as a result, MgH_2 was produced as a byproduct. It was concluded that the maximum hydrogen capacity would be 8.3 wt%.[76]

Rönnebro, Ewa, et al. successfully synthesized $Ca(BH_4)_2$ (See Figure 3) without producing byproducts by reacting a ball-milled mixture of calcium hexabromide ($CaBr_6$) and calcium hydride (CaH_2) in a 1:2 M ratio under 700 bar hydrogen pressure and a temperature range of 400 °C–440 °C. The reversible hydrogen storage capacity was estimated to be 9.6 wt%.[77]

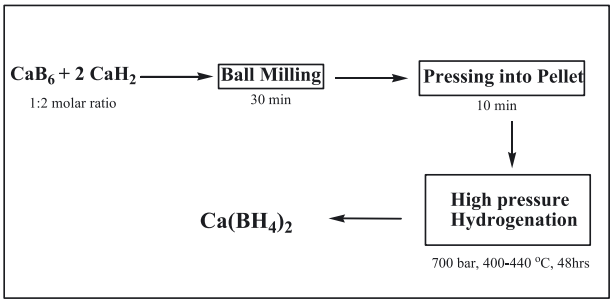

Figure 3: Schematic representation of the formation $Ca(BH_4)_2$ without byproduct.

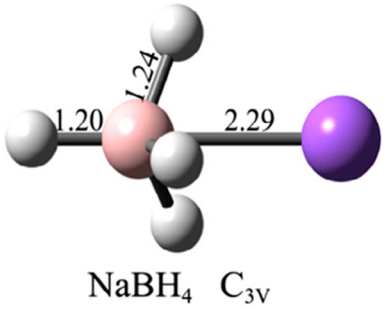

Figure 4: Crystal structure of $NaBH_4$ compound.[70]

Matsunaga, Tomoya, et al. developed magnesium borohydride $Mg(BH_4)_2$ with a 14.9 wt% hydrogen content. They looked into the possibility of creating Mg $(BH_4)_2$ by reacting lithium borohydride with magnesium chloride. At temperatures higher than 532 K and hydrogen pressure of 10 MPa, the reaction occurs. Lithium chloride and magnesium borohydride was the end products.[78]

Despite recent advancements in regenerating metal borohydrides via hydrolysis, a significant challenge remains: the need for additional water during the hydrolysis process to reduce system density, limiting its use in mobile applications.[79] The advancements in research on the pyrolysis of metal borohydride such as $NaBH_4$, KBH_4, $LiBH_4$, $Ca(BH_4)_2$ and other have been reviewed. Table 1 includes the dehydrogenation products, the temperatures at which they occur, and theoretical hydrogen desorption ratios of some of these borohydrides.

2.2.1 Bimetal-borohydrides materials

Bimetal-borohydrides are compounds made up of borohydride anions (BH4-) paired with two distinct metal cations. These materials are highly significant in material science, especially for their promising uses in storage of significant amount of hydrogen, catalysis as well as other energy technologies because of having high content of hydrogen.[88] Kim, Chul et al., investigated the process of formation, properties of structure, thermodynamic durability and reaction properties of $LiSc(BH_4)_4$ utilizing multinuclear NMR analysis as well as DFT computations in order to evaluate its possible usage in hydrogen storage devices.[89] Nakamori et al., proposed initially the mechanochemical production of $Sc(BH_4)_3$[90,91] was later claimed to actually produce $LiSc(BH_4)_4$, according to findings by Hwang and colleagues[92,93] and also the research team of Hagemann.[94] Some samples made by ball-milling combinations of $ScCl_3$ & $LiBH_4$ in different ratios that are varied from 1:3 to 1:6 were examined by the team Kim, Chul et al. They also found the

Table 1: Hydrogen storage properties of several single metal-borohydrides.

Metal borohydrides	Products	Dehydrogenation temperature	Hydrogen proportion	ΔH KJ/mol H_2	R.f
$LiBH_4$	LiH, B, H_2	268–492 °C (peak at 370 °C)	13.8 wt%	74	73,80–82
$NaBH_4$	NaH, B, H_2	150–390 °C	7.9 wt%	75	83,84
	Na, H	>440 °C	2.7 wt%		
$Ca(BH_4)_2$	CaH_2, B, H_2	400–440 °C	9.6 wt%	36	77
KBH_4	KH, $K_2B_{12}H_{12}$, H_2	>284 °C	4.0 wt%	–	85
	KH, B, H_2	>498 °C	4.6 wt%		
$Mg(BH_4)_2$	MgH_2, B, H_2	230 °C	14.9 wt%	39.3	86,87

results of phases utilizing the information from X-ray diffraction as well as NMR spectra (^{45}Sc, ^{11}B, and ^{6}Li). Additionally, first-principles calculations were conducted to explore both $Sc(BH_4)_3$ and $LiSc(BH_4)_3$ ground-state characteristics and structures.

The breakdown and hydrogen release patterns of these compounds were theoretically forecasted. Furthermore, $LiSc(BH_4)_4$ was experimentally analyzed after it had undergone hydrogen absorption and release processes. Furthermore, they concluded that at 400 Celsius temperature and approximately 70 bar of hydrogen gas pressure, hydrogen absorption took place.[89] Hydrogen was released at a temperature of 400 °C inside a stainless-steel reactor, which was initially evacuated and then pressurized from 1 to 3 atm of H_2 gas. This setup was consistent with previous descriptions.[95] Recently, Hagemann and colleagues determined the crystalline structure of $LiSc(BH_4)_4$ through mechanochemical methodology. They also assigned the structure to $P\bar{4}2c$ space group through HR-SXRD analysis.[94] Kim et al. employed the PEGS algorithm to identify a low-energy configuration of LiSc(BH4)4. This structure is notable for its high symmetry, which was classified under the **I4j (#84)** space group. In this context, **I4j** indicates a tetragonal crystal system with body-centered symmetry (**I**), a fourfold rotational axis (**4**), and specific inversion or reflection symmetry (**j**), and the space group (**#84**) is a specific identifier for this highly symmetrical structure in their analysis. Further, the arrangement, estimated by PEGS to have the highest symmetry as well as lowest energy, aligns with the I4j structure as presented in their analysis. (see Figure 5).[89]

Morten b. Ley et al. synthesized hydrogen storage materials, $LiLa(BH_4)_3Cl$ and $LiGd(BH_4)_3Cl$, using a mechanochemical method involving MC_3 (M = La, Gd) and $LiBH_4$. The Gd-containing compound required annealing for stabilization. Both materials showed high hydrogen content for example $LiLa(BH_4)_3Cl$ contains 5.36 wt% H_2, and $LiGd(BH_4)_3Cl$ contains 4.95 wt% H_2. Further, they showed good lithium-ion conductivity, making them good for hydrogen storage. The structure analysis revealed a cubic crystal system with an altered cubane core structure, and decomposition occurred at

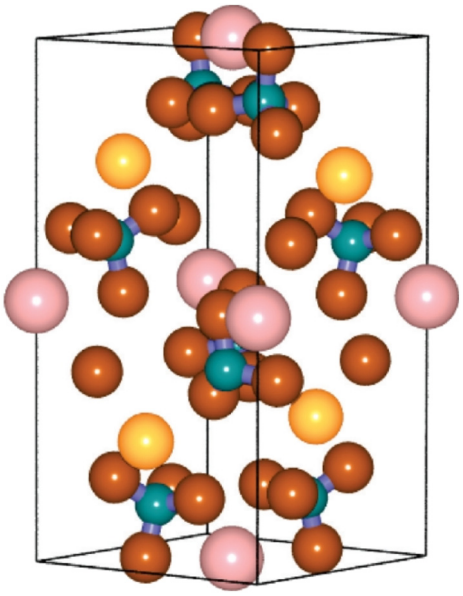

Figure 5: The depiction of tetragonal arrangement of the compound $LiSc(BH_4)_4$ in I4j (#84) space group. Sc and Li atoms are represented by gold color.[89]

300 °C, producing metal borides/hydrides and LiCl.[96] Nguyen et al., (2018) synthesized $LiCe(BH_4)_3Cl$ (M = La, Ce, Gd) via ball-milling and annealing. $LiCe(BH_4)_3Cl$ exhibited strong stability and was tested as a solid electrolyte in Li–S batteries, showing a promising discharge capacity of 1,186 mA h/g with a retention of 510 mA h/g following nine cycles, proving its potential for solid-state electrolyte applications in energy storage systems.[97] The compounds $LiGd(BH_4)_3$ and $LiLa(BH_4)_3Cl$ having same structure to that of $LiCe(BH_4)_3Cl$ previously studied.[98] These two substances feature a distorted cubane-shaped M_4Cl_4 core[99] and consist of distinct anionic clusters, $[M_4Cl_4(BH_4)_{12}]^{4-}$ (where M = La or Gd). These clusters are balanced by Li^+ ions to maintain the overall change balance the structure. In $LiLa(BH_4)3Cl$, the bond angles between B–La–B is approximately 99.4° and 73.1° between Cl–La–Cl. La–Cl distance is measured at 2.987 Å, while La–B distance measured 2.73 Å. For $LiGd(BH_4)_3Cl$, the corresponding bond

angles B-Gd-B and Cl-Gd-Cl are normally different, measured at 98.6° and 73.2°, with the Gd–B and Gd–Cl distances being 2.61 Å and 2.880 Å. These small variations reflect differences in the atomic sizes and bonding environments of La and Gd within their respective crystal structures.[96] Figure 6 presents the crystal structure of $LiLa(BH_4)_3Cl$ and $LiGd(BH_4)_3Cl$.

2.3 Alanates

These are complex metal hydrides consists of aluminum, and one or more alkali or alkaline earth metals, like lithium or sodium. Examples include sodium alanate ($NaAlH_4$) and lithium alanate ($LiAlH_4$). These materials are highly valued to store hydrogen, because these substances can release and absorb hydrogen reversibly under specific conditions. The hydrogen storage process in alanates involves decomposition reactions, during which hydrogen gas is released when heat is applied. For example, sodium alanate undergoes a series of decomposition steps to release hydrogen at moderate temperatures. These unique characteristics position alanates as potential materials for lightweight and effective hydrogen storage in fuel cell technologies. However, challenges like improving reaction rates and ensuring thermodynamic stability must be overcome for their widespread application.[100–102] Sodium alanate ($NaAlH_4$) was initially produced by reacting sodium hydride (NaH) with either aluminum bromide ($AlBr_3$) or aluminum chloride ($AlCl_3$) in tetrahydrofuran (THF) solution.[103]

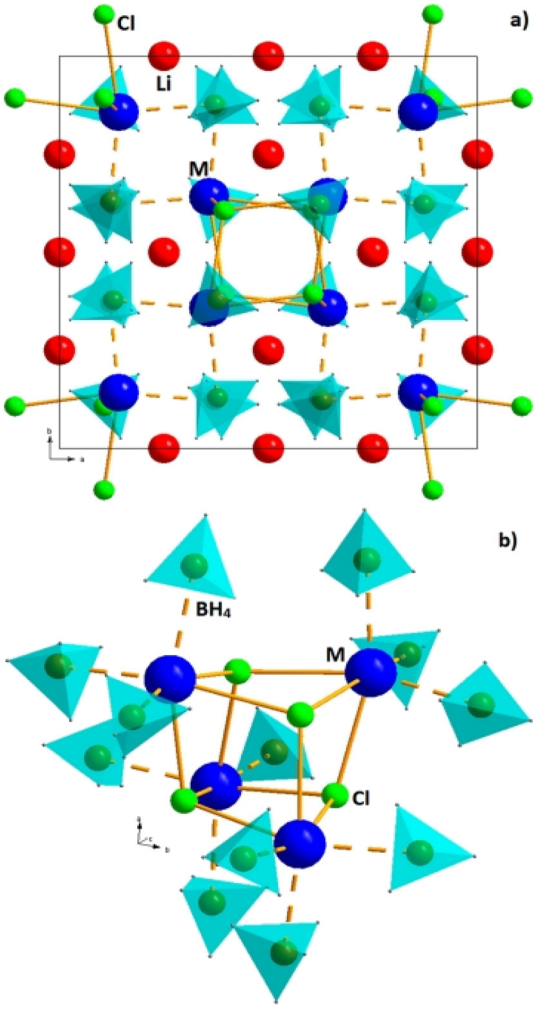

Figure 6: Crystal structure of $LiLa(BH_4)_3Cl$ and $LiGd(BH_4)_3Cl$. Part (a) depicts the crystal structure of both compounds of $LiM(BH_4)_3Cl$ (M = Gd & La). Part(b) represents the structure of $[M_4Cl_4(BH_4)_{12}]^{4-}$ where M = La or Gd with M_4Cl_4 distorted cubane core.[96]

3 Perovskite compounds for hydrogen storage

Perovskite hydrides certainly show promise for hydrogen storage applications given their high gravimetric hydrogen density, which in some cases exceeds 5 wt% and even approaches 8 wt%. While recognized for outstanding hydrogen uptake, these materials have thus far only scratched the surface of their potential. Optimization of syntheses and crystal structures may unravel secrets that further increase storage capacities. Structural tuning could allow perovskites to saturate more fully with hydrogen, packing even denser energies into their intricate frameworks. Unexpected compositions may also reveal themselves through innovative screening techniques. With continued advances in synthesis and characterization, perovskite hydrides could fulfil their role as leading candidates for onboard hydrogen storage.[5,104] The general procedure for harnessing perovskite compounds in hydrogen storage involves several key steps. Firstly, perovskite materials such as ABO_3 are synthesized through solid-state approaches or solution-based techniques, ensuring optimal structural qualities. These materials are then exposed to hydrogen fuel under significant pressure, allowing hydrogen to be absorbed into the perovskite lattice structure. The absorbed hydrogen is stored within the complex crystal structure, delivering stable and high-capacity storage. When necessary, heat or decreased pressure induces dehydrogenation, liberating hydrogen gas molecules. The processes of hydrogen absorption and the subsequent release of hydrogen can be repeated multiple times, with perovskite compounds exhibiting long-term stability and cycling capability when modified or doped to improve their reaction kinetics and uptake properties. (see Figure 7). Perovskite hydrides showcase a

flexible approach for diverse hydrogen storage applications. For fuel cell automobiles, they can function as stable storage platforms to safely and productively retain hydrogen, energizing hydrogen fuel cells for transportation purposes. When it comes to renewable energy storage, perovskites offer an effective strategy for retaining excess hydrogen created from solar or wind power. This hydrogen can then be used during moments of low energy generation, boosting the dependability of renewable energy infrastructure. In portable power gadgets, perovskites supply a compact and productive storage solution for small-scale uses such as portable power units or emergency power supplies. Additionally, perovskite hydrogen storage is being explored for stationary energy systems in large-scale settings, such as energy plants and industrial environments, where they can retain significant amounts of hydrogen for long-term energy storage and utilization.

Recently, perovskite-type metal hydrides (ABH_3) have gained interest as hydrogen storage materials due to their significant hydrogen storage capacity.[105,106] The usual arrangement and structure of perovskite compounds is ABX_3, where X shows an anion and B as a cation. Scientists have focused on Mg-based perovskite hydrides, especially $NaMgH_3$, because of their remarkable hydrogen holding properties.[107,108]

In 2024, Al, Selgin et al., studied MgX_3H_8 where X = Sc, Ti, Zr for their hydrogen holding capability. The researchers claimed that these types of materials are excellent for storing hydrogen in solid form. The crystal structure representative of MgX_3H_8 (X = Sc, Ti, Zr)[109] and Li_2CaH_4 and Li_2SrH_4 hydrides[110] are displayed in Figure 8. Debye vibrational energy, vibrational free energy, entropy, and heat capacity are shown in the graphs of Figure 9. These properties are the means for the substance to respond to temperature changes. Debye vibrational energy measures the energy needed for atomic relaxations, whereas vibrational free energy shows how much extra storage or release of power there is in material. Entropy refers to the disorder of the system, which increases with temperature, and heat capacity is a measure of how much heat can be absorbed before significant temperature changes occur. Comparison of these properties among Sc, Ti, and Zr helps to elucidate their influence on a material's thermal behaviour, vital for such applications as hydrogen storage technology. To explore the substances for the storage of solid-state hydrogen, the GDH were computed for MgX_3H_8 (X = Sc, Zr and Zr) as similar to both Li_2CaH_4 hydride and Li_2CaH_4 hydrides.[110,111]

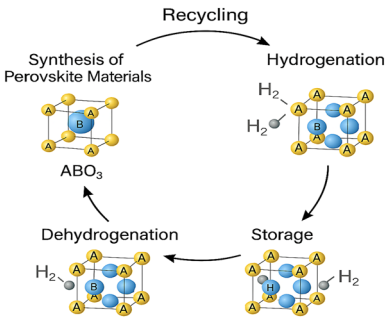

Figure 7: General schematic representation of hydrogenation/dehydrogenation of perovskite compound.

$$C_{wt\%} = \left(\frac{\left(\frac{H}{M}\right) M_H}{M_{Host}\left(\frac{H}{M}\right) M_H} \times 100 \right)\% \quad (1)$$

The above equation (1) was used to determine the GDH, which came out to be 4.60 wt percent for $MgSc_3H_8$, 2.56 wt percent for $MgZr_3H_8$, and 4.38 wt percent for $MgTi_3H_8$. Additionally, they also determined the GDH values for Li2CaH4 as well as LiSrH4 which were −6.95 wt% and 3.83 wt%, respectively. In terms of practical hydrogen storage applications, these computed values are near the 4.5 wt% goal established by the Department of Energy of United state.[113,114] To verify the feasibility of synthesis and the thermodynamic stability of MgX_3H_8 (where X = Sc, Ti, Zr), the formation enthalpy has been calculated as follows eq(2).[115]

$$\Delta E_f = E_{T\,(MgX3X8)} - \left(E_{Mg} + 3E_x + 4E_{H2}\right) \quad (2)$$

In the provided equation, $E_{T(MgX3H8)}$ represents the total energy of the compound MgX_3H_8 (where X = Sc, Ti, Zr), while E_{Mg}, E_X, E_{H2} denote the ground state total energies of magnesium (Mg) atoms, X atoms (Sc, Ti, or Zr), and hydrogen (H_2) molecules, respectively. The calculated formation enthalpies for the proposed materials are presented in Table 2. These substances are thermodynamically and synthetically stable because the results also showing that they have negative

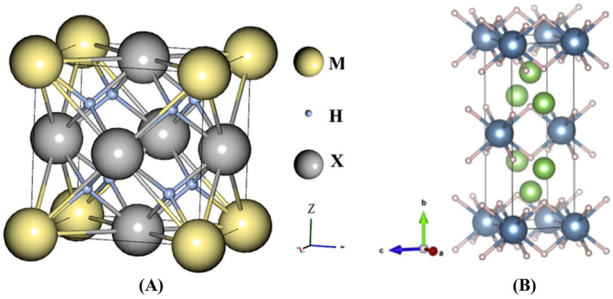

Figure 8: Crystal structure representative of MgX_3H_8 (X = Sc, Ti, Zr) and Li_2CaH_4 and Li_2SrH_4 hydrides. (A) The crystal structures representatives of MgX_3H_8 (X = Sc, Ti, Zr) and (B) Li_2CaH_4 and Li_2SrH_4. DFT-optimized crystal structures of Li_2XH_4, (X ¼ Ca, Sr). Green ball for Li, blue for Ca (or Sr) and white ball for hyShear modulus (G)shear modulus (G)shear modulus (G) shear modulus (G)shear modulus (G)shear modulus (G)shear modulus (G) shear modulus (G)drogen atom).[112]

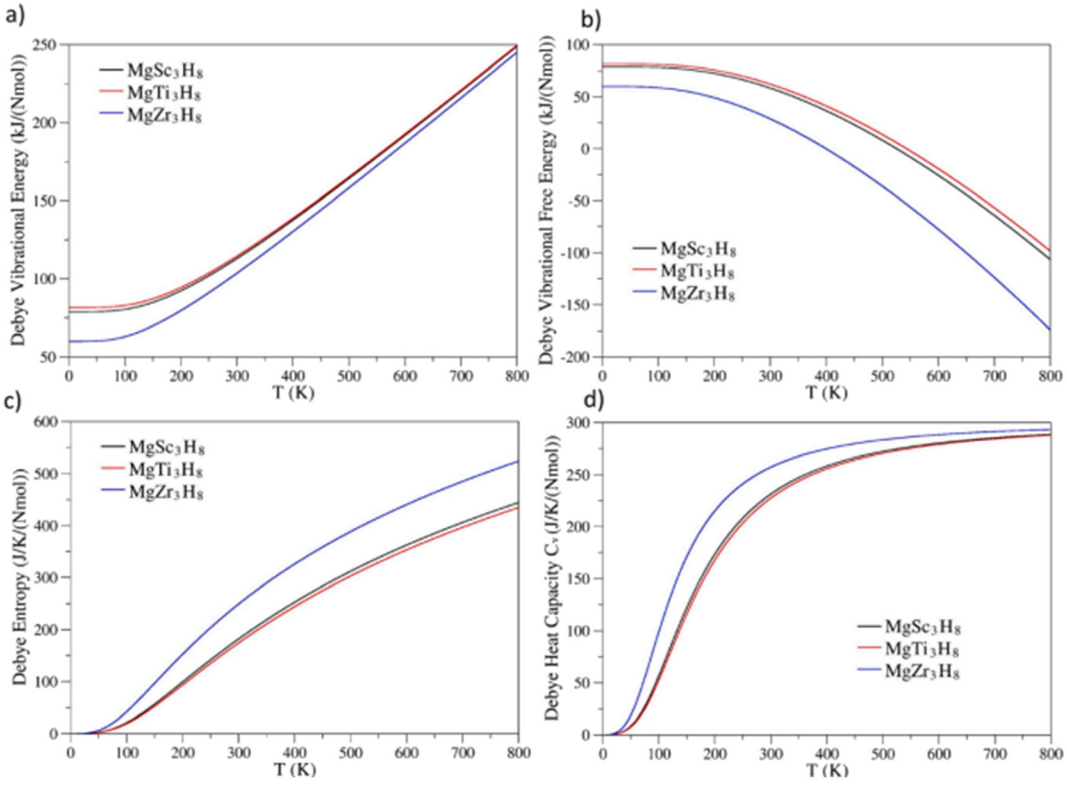

Figure 9: Illustration of thermodynamic properties such as Debye vibrational energy, vibrational free energy, entropy, and heat capacity of the compounds of MgX_3H_8 (X = Sc, Zr, Ti).[112]

formation enthalpies.[116] Various properties, such as physical and mechanical, were also computed as shown in Table 2.

Perovskite materials are ceramics and are known for being hard, making them potential candidates for solid-state hydrogen storage. However, there's limited research on their hydrogen storage capabilities, with only a recent study exploring $MgTiO_3H_x$ and $CaTiO_3H_x$ compounds.[117] Gencer, Aysenur et al. used first principal calculation to study a novel perovskite substance $CaTiO_3H_x$ as well as $MgTiO_3H_8H_x$ (where x = 0,3,6 and 8). They found that all substances had stability, but $MgTiO_3H_6$ and $MgTiO_3H_8$ were unstable. $MgTiO_3$, $CaTiO_3$, and $CaTiO_3H_6$ were determined to be energetically and mechanically stable, with $MgTiO_3$ and $CaTiO_3H_6$ being ductile and $CaTiO_3$ being brittle. The metallic characteristic of $MgTiO_3$ and the semiconductor properties of $CaTiO_3$ and $CaTiO_3H_6$ were revealed by electronic band structure with 1.89 eV band gap for $CaTiO_3$ and 1.23 eV band gap for $CaTiO_3H_6$. Furthermore, the study revealed that the compound $CaTiO_3H_6$ has 821.1 K desorption temperature and 4.27 wt% for their hydrogen holding capacity.[117]

Equation (1),[111] can be utilized to determine the gravimetric hydrogen holding capability, which is the total quantity of hydrogen saved per unit mass of materials. Figure 10 shows that the materials, such as $MgTiO_3Hx$ and $CaTi_3Hx$ (X = 0,6,8), have cubic structures. (space group: 221, *pm*3*m*). They also investigated $BaYO_3$ Perovskite for holding hydrogen using DFT. The study revealed that $BaYO_3H_3$ is stable, with 1.09 wt% hydrogen holding or storage capacity. In contrast, $BaYO_3H_9$ was found to be unstable and not good for hydrogen storage because of its positive formation energy.[118]

Hydrogen bonding research studies can be carried out after determining the main physical characteristics of the cubic phase of $BaYO_3$, which was chosen for its durability as well as tiny volume. The cubic phase (221, Pm-3m) has Ba at 1b, Y at 1a, and O at 3d Wyckoff positions, with hydrogen added at 3c, forming $BaYO_3H_3$. The structure is shown

Table 2: Calculation of bulk modulus (B), shear modulus (G), B/G ratio, poisson's ratio (σ). Young modulus (E), and formation enthalpy (ΔH_f, eV/atom) for MgX_3H_8 (X = Sc, Ti, Zr) and Li_2CaH_4 and Li_2SrH_4 hydrides.

Materials	B/G ratios	(G,Gpa)	(E,Gpa)	(σ)	ΔH_f, eV/atom
$MgSc_3H_8$	1.697	50.247	125.998	0.25	−0.324
$MgTi_3H_8$	1.789	59.641	150.832	0.26	−0.327
$MgZr_3H_8$	1.762	57.206	144.323	0.26	−0.411
Li_2SrH_4	1.341	26.325	63.255	0.201	2.492
Li_2CaH_4	1.278	29.569	70.361	0.189	2.551

inFigure 11a. Additionally, after the determination of lattice constant was 4.55 Å, optimizing the structure and formation energy (–0.81 eV/atom) demonstrated that the compound $BaYO_3H_3$ is synthesizable and stable. For the compound, the cohesive energy was also computed by using equation (3) which was **-1.10** eV/atom.

$$E_{\text{cohesivve}} = \frac{E_{BaYO_3H_3} - E_{BaYO_3}}{3} \quad (3)$$

$BaYO_3H_3$ has been optimized and determined to be stable and synthesizable. Hydrogen storage materials must meet specific criteria, one of which is gravimetric hydrogen storage capacity. This capacity shows how much hydrogen quantity can be stored in 1 unit mass of the substance. The formula $BaYO_3H_9$ was derived by adding up to 6 hydrogen atoms to $BaYO_3H_3$ at 6e Wyckoff positions. Its crystal structure, shown in Figure 11b, has a lattice constant of approximately 5.97 Å and a formation energy of 0.35 eV. Due to its instability and positive formation energy, $BaYO_3H_9$ is unsuitable for hydrogen storage materials.[119]

In 2017, Bilal Rehmat et al.[120] used DFT (Density Function theory) to explore the physical and mechanical characteristics of the compounds $NaBeH_3$ and $LiBeH_3$, along with their orthorhombic and cubic phases. WIEN2k code was applied to estimate the band gaps, and both hydrides were confirmed to be mechanically stable. They computed various mechanical properties, i.e., bulk, shear, and Young's modulus, as well as elastic constants, micro-hardness, and Poisson's ratio, which were also determined. The obtained values were found to be higher than those of other commonly studied hydrides for hydrogen storage. With a B/G ratio under 1.75, both $LiBeH_3$ and $NaBeH_3$ were categorized as brittle. Furthermore, the hydrides showed significant anisotropy, and their calculated Debye temperatures – reflecting strong atomic bonding and robustness – were higher compared to $NaMgH_3$, $KMgH_3$, and $LiBH_4$. $LiBeH_3$ was first prepared by Bell et al.[121] Tamassy-Lentei et al. studied the structure and stabilities of $LiBeH_3$ by the theoretical ab-initio method.[122] The perovskite structure of $LiBeH_3$ was also analyzed by Gupta et al.[123] and Seel et al.[124] Gupta et al. declared that it behaves as a semiconductor at 0.21 eV energy gap, while Seel's indicated that it has the highest energy gap of 11 eV due to this; it behaves like an insulator.

Ming et al.[125] and Xiao-Jiao et al.[126] investigated the electronic characteristics of $LiBeH_3$ cubic perovskite. Hu et al.[127] Identified a monoclinic structure with a 4.84 eV band gap and determined its enthalpy of formation. In another investigation, Hu et al.[128] determined the behavior of $LiBeH_3$ under high pressure conditions. Blanca[129] recently refined the perovskite structure and estimated a band gap of 1.275 eV. Additionally, Boettger studied a 3-Layer film of $LiBeH_3$ and found it to display weak metallic properties.[130]

According to Vajeeston et al. ,[131] NaBeH3 takes on a cubic CaTiO3-like structure with symmetry Pm3 m. In their broader

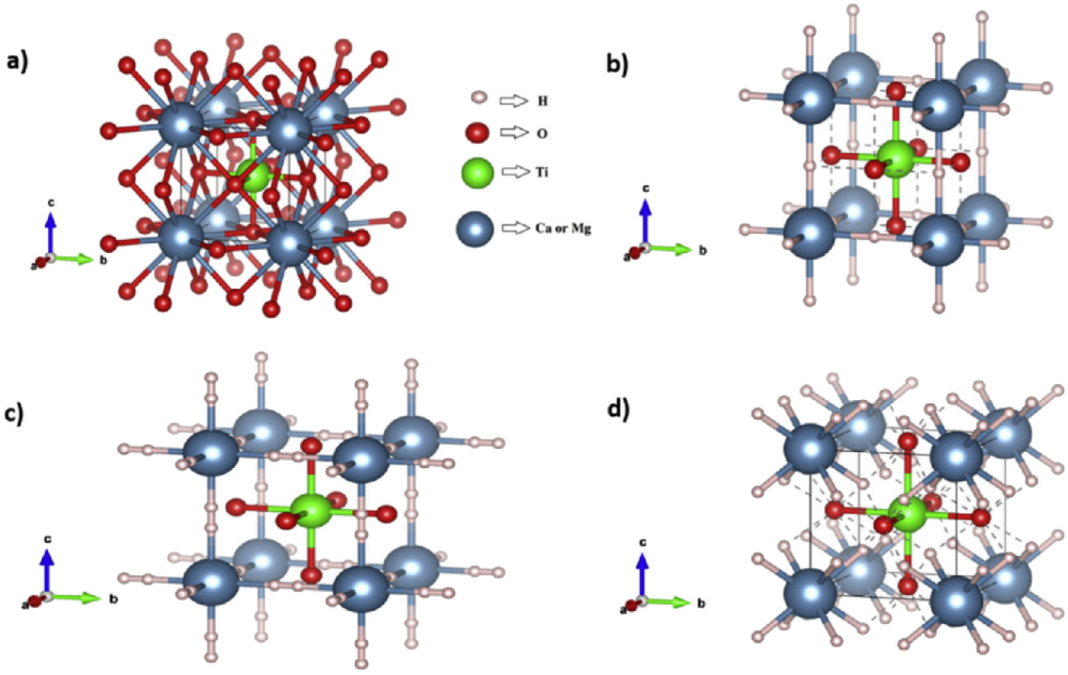

Figure 10: The figure shows the crystal structures of the compounds (a) $ATiO_3$, (b) $ATiO_3H_3$, (c) $ATiO_3H_6$, and (d) $ATiO_3H_8$, where "A" denotes either a magnesium (Mg) or calcium (Ca) atom. These structures illustrate the stepwise inclusion of hydrogen in the $ATiO_3$ lattice.[117]

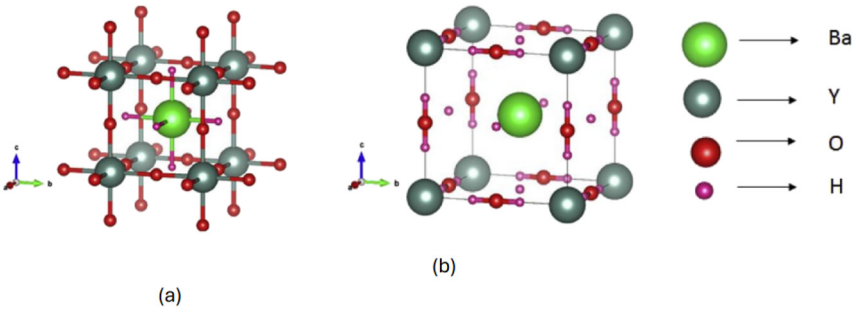

Figure 11: Crystal structure of $BaYO_3H_3$ (a) and $BaYO_3H_9$ (b).[118]

investigation, Vajeeston et al.[132] applied DFT to study both LiBeH3 and NaBeH3, revealing that LiBeH3 forms an orthorhombic (*Pnma*) structure while NaBeH3 adopts a cubic perovskite structure. Both compounds were characterized as strong insulators. Karazhanov et al.[133] explored the possibility of achieving n-type and p-type conductivity in $NaBeH_3$. Furthermore, Sanchez-Castro et al.[134] conducted comprehensive electronic and structural evaluations of the two materials. For the first time, the elastic constants of cubic and orthorhombic $LiBeH_3$, as well as cubic $NaBeH_3$, were determined utilizing the DFT method. A variety of exchange-correlation functionals were used. Young's, bulk, and shear modulus, as well as Poisson's ratio and Debye temperature, were also calculated.[120] Their calculations involved two crystal structures for LiBeH3. The first structure is an orthorhombic perovskite (space group *Pnma*, No. 62), comprising a unit cell with 20 atoms. [132] The 2nd Structure examined is a cubic perovskite (space group Pm3 m, No. 221) consisting of a unit cell with 5 atoms.[126]

In cubic perovskite structures, the atomic positions are arranged as follows: for $LiBeH_3$, Li is located at (0,0,0), Be at (1/2, 1/2, 1/2), and H at (0, 1/2, 1/2). In the case of $NaBeH_3$, Be occupies (0,0,0), Na is at (1/2, 1/2,1/2), and H is positioned at (0, 0, 1/2). All these structures are illustrated in Figure 12.[120]

In 2023, Aman Rafique et al. studied the physical properties and hydrogen storage characteristics of $XCoH_3$ (where X = In, Mn, Sn, Cd) through first-principles calculations. The materials are found to be stable and exhibit metallic behavior with zero-band gap. Most compounds are ductile, although $MnCoH_3$ and $SrCoH_3$ display brittleness. $CdCoH_3$ is noted as the hardest material, while $SrCoH_3$ shows superior photon absorption, and $SnCoH_3$ is effective at reflecting radiation. The gravimetric hydrogen storage capacities are recorded at 1.71 %, 2.59 %, 2.03 %, 1.68 %, and 1.74 wt% for $InCoH_3$, $MnCoH_3$, $SrCoH_3$, and $CdCoH_3$, respectively. Due to its higher gravimetric ratio. $MnCoH_3$ is recommended as the most favorable material for hydrogen storage.[135] The analysis focuses on the structural characteristics of $XCoH_3$ (X = In, Mn, Sr, Sn, Cd) hydride perovskites. The phase of these materials is identified using the tolerance factor. The value between 0.9 and 1.0 indicates that the perovskite adopts a cubic structure.[136] Tolerance factors were also calculated for InCoH3, MnCoH3, SrCoH3, SnCoH3, and CdCoH3 are 0.98, 0.95, 0.93, 0.97, and 0.96, respectively. These values confirm that all these hydride perovskites possess a cubic structure, with a space group designation of pm3m (221), as depicted in Figure 13. Evaluating the stability of a crystal structure is crucial in research, so the thermodynamic and dynamic stability of these compounds was assessed through formation energy and phonon spectra, respectively.[135] Additionally, the formation enthalpy of each compound was determined using the following equation (4).[136]

$$\Delta H^{\mathrm{XCoH3}} = E_t^{\mathrm{XCoH3}} - \left[E_t^X + E_t^{Co} + 3E_t^H\right] \quad (4)$$

Nanlin Xu et al. (2023) studied a novel type of perovskite hydrides XVH_3 (where X = Na, K, Cs, Rb) for the properties of hydrogen storage utilizing DFT calculations. The research demonstrates that XVH3 compounds exhibit both thermodynamic and mechanical stability, supported by formation energy and elastic constant calculations. Their B/G ratio indicates brittleness, with a bonding nature closer to ionic. These hydrides act as insulators with ferromagnetic behavior, while Bader charge analysis highlights their charge transfer properties. Optical assessments show high UV absorption, and phonon dispersion analysis confirms their dynamic stability. At different temperatures, various thermodynamics properties, including heat capacity, free energy, and entropy, were calculated. The hydrogen storage capacities were calculated as 3.78 wt% for $NaVH_3$, 3.15 wt% for KVH_3, 2.12 wt% for $RbVH_3$, and 1.59 wt% for $CsVH_3$ as shown in Table 3, along with other properties. This study introduces new perovskite hydrides as outstanding materials for the storage of hydrogen.[137] Figure 14 shows that the XVH_3 compound belongs to the space group PM-3M (221). The Wyckoff positions for the atoms are X at 1a (0, 0, 0), V at 1b (0.5, 0.5, 0.5), and H at 1c (0, 0.5, 0.5). Structural optimization was performed to determine the ground state configuration of XVH_3 using the Birch-Murnaghan method, represented by the following equation.[138]

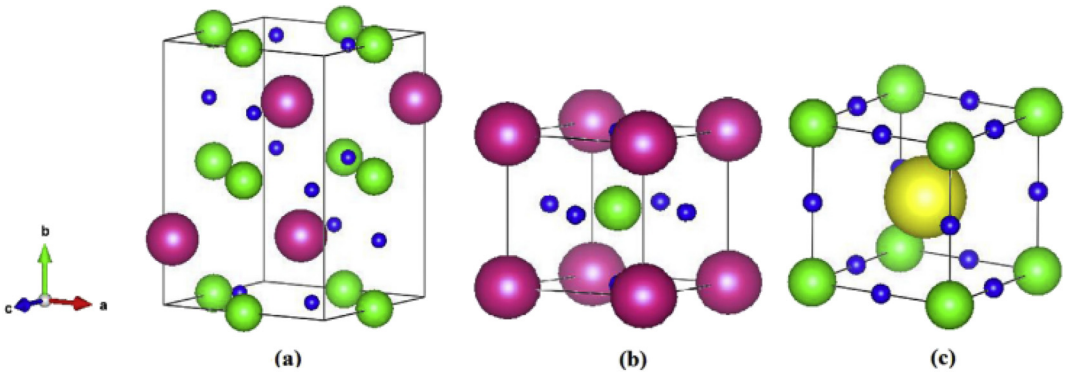

Figure 12: Crystal structures of (a) orthorhombic $LiBeH_3$, (b) cubic $LiBeH_3$, and (c) $NaBeH_3$ are depicted. In the illustrations, lithium (Li) is represented in large pink spheres, beryllium (Be) in medium green spheres, hydrogen (H) in small blue spheres, and sodium (Na) in large yellow spheres.[120]

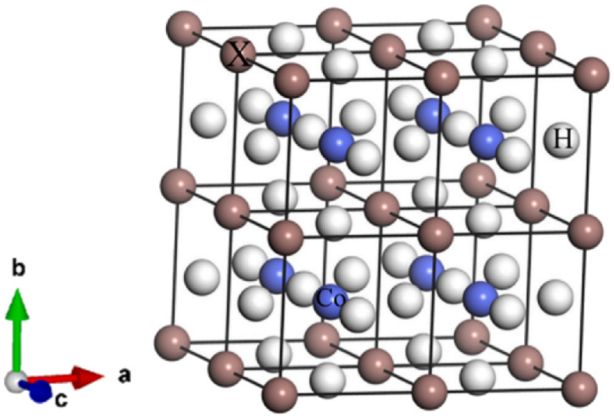

Figure 13: Structure for $XCoH_3$ (X = Mn, Sr, Sn, In, and Cd). White balls represent hydrogen (H) atoms, blue balls represent cobalt (Co) atoms, and brown balls represent metal atoms (X), where X can be Mn, Sr, Sn, In, or Cd.[135]

Siddique et al.[140] analyzed the hydrogen storage properties of compound $LiVH_3$, which was 4.8 wt%. Furthermore, they also studied $AeVH_3$ (A = Be, Mg, Ca, Sr) compounds for hydrogen storage and found that these compounds having 4.6, 3.7, 3.1, and 2.0 wt% hydrogen storage capacity, respectively.[141]

In 2018, Abdullah Candan et al.[139] studied MgXH3 (X = Fe, Co) for hydrogen storage. Both compounds showed mechanical stability, with MgFeH3 identified as brittle and MgCoH3 as ductile. Key properties, such as lattice constants (a_0), bulk modulus (B), shear modulus (G), and elastic constants (C_{11}, C_{12}, C_{44}) were analyzed. Figure 15a depicting the cubic structure for MgXH3 (X = Fe, Co), with lattice constants of 3.280 Å for MgFeH3 and 3.288 Å for MgCoH3, as listed in Table 3.

In 2020 M. Garara et al.[142] also investigated a new perovskite-type compound, $MgCoH_3$, for hydrogen storage properties. They also investigated its crystal structure, stability, and kinetic properties etc., using DFT calculation. The phonon frequencies and thermal properties were determined by DFT techniques and utilizing the QE code alone with phonopy software[138[143] $MgCoH_3$, a bulk perovskite hydride, crystallizes in a body-centered cubic (BCC) structure under the space group Pm-3m (No.221). The unit cell consists of five atoms: magnesium is positioned at the corner

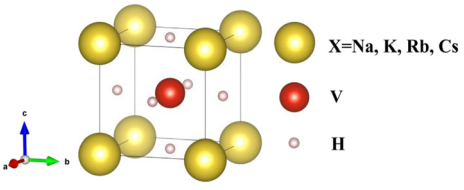

Figure 14: Structure of cubic XVH_3 where X = Na, K, Cs.[138]

Table 3: Calculated properties (lattice constant, Young's, shear, and bulk modulus, anisotropy, Poisson's ratio, and hydrogen storage capacity (wt%) for the compounds $MgXH_3$ and XVH_3.

Compounds	(æ)Å	B(GPa)	G(GPa)	B/G	E(GPa)	A	*v*	Cwt%/wt%	References
$MgFeH_3$	3.280483	131.39	75.86	1.73	190.84	0.53	0.258	–	139
$MgCoH_3$	3.288151	126.36	66.68	1.90	170.11	0.54	0.276	–	139
$NaVH_3$	3.710	54.155	41.780	1.336	100.328	0.641	0.200	3.78	138
KVH_3	3.912	48.505	39.971	1.222	94.217	1.032	0.179	3.15	138
$RbVH_3$	4.022	45.001	36.352	1.243	85.949	1.265	0.183	2.12	138
$CsVH_3$	4.166	40.535	31.670	1.291	75.507	1.511	0.192	1.59	138

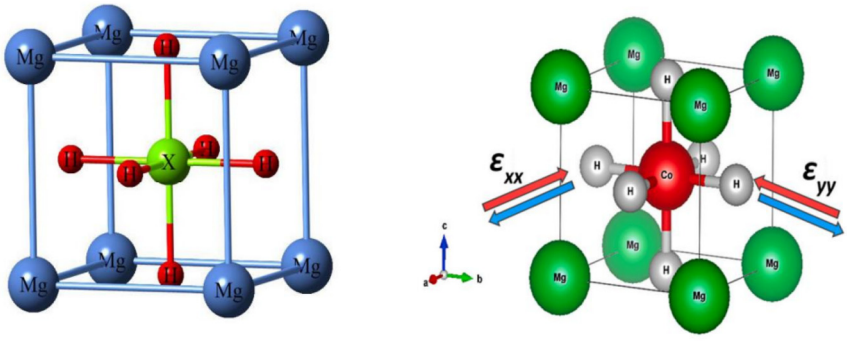

Figure 15: Crystal structure of $MgXH_3$ (X = Fe, Co) and $MgCoH_3$. (a) $MgXH_3$ (X = Fe, Co).[139] (b) $MgCoH_3$.[142]

(0, 0, 0), cobalt occupies the center, and three hydrogen atoms are placed at octahedral positions on the face center, with coordinates (0.5, 0.5, 0.0), (0.5, 0.0, 0.5) and (0.0, 0.5, 0.5). The relaxed structure yields a lattice parameter of 3.278 Å, which is consistent with prior research findings.[139,144,145, Figure 15b showing the crystal structure for $MgCoH_3$.

4 Conclusions

Hydrogen has long been recognized as a key element in the transition to sustainable and clean energy, especially with its increasing role in fuel cells and energy storage systems. As demand for hydrogen rises across various applications, efficient storage solutions are becoming increasingly vital. This review highlights the crucial role of advanced materials in the efficient storage of hydrogen, a key element in the transition to sustainable energy. The main findings of this study emphasize the significant potential of metal hydrides, perovskite compounds, and other promising materials for hydrogen storage, addressing both their hydrogen holding capacity and desorption properties. Materials such as magnesium hydrides (MgH_2), titanium hydrides (TiH_2), and perovskite hydrides like $NaVH_3$ and MnCoH3 have demonstrated excellent hydrogen storage capacities, with $NaVH_3$ showing the highest at 3.78 wt%. Additionally, the compound $CaTiO_3H_6$, with a desorption temperature of 821.1 K and a hydrogen holding capacity of 4.27 wt%, is identified as a promising material for further research. This study claims that integrating computational tools such as Density Functional Theory (DFT) plays a pivotal role in understanding the behavior of these materials in hydrogen storage scenarios. Furthermore, the review underscores the importance of both thermodynamic and mechanical properties, such as mechanical stability and elasticity, which are critical for real-world applications. This topic is of paramount importance as hydrogen is increasingly seen as a key element for sustainable and clean energy production. Efficient hydrogen storage is essential to realize the full potential of hydrogen as a clean energy source. The research gap filled by this study includes the lack of detailed comparison across various materials, limited understanding of material behavior in hydrogen storage applications, identification of underexplored materials, and the integration of mechanical and thermodynamic properties in evaluating storage materials. By addressing these gaps, this review contributes valuable insights to guide future research and development in the field of hydrogen storage.

Acknowledgment: Not applicable.
Research ethics: Not applicable.
Informed consent: Not applicable.
Author contributions: All authors contributed equally.
Use of Large Language Models, AI and Machine Learning Tools: Large Language Models (LLMs), including ChatGPT by OpenAI, were used to assist with language editing, grammar checking, and paraphrasing of certain text sections. These tools were not used for data analysis or generating original research content.
Conflict of interests: Not applicable.
Research funding: Not applicable.
Data availability: Not applicable.

References

1. Lykas, P.; Georgousis, N.; Bellos, E.; Tzivanidis, C. A Comprehensive Review of Solar-Driven Multigeneration Systems with Hydrogen Production. *Int. J. Hydrogen Energy* **2023**, *48* (2), 437–477.
2. Zhu, Z.; Jiang, T.; Ali, M.; Meng, Y.; Jin, Y.; Cui, Y.; Chen, W. Rechargeable Batteries for Grid Scale Energy Storage. *Chem. Rev.* **2022**, *122* (22), 16610–16751.

3. Baldi, F.; Coraddu, A.; Kalikatzarakis, M.; Jeleňová, D.; Collu, M.; Race, J.; Maréchal, F. Optimisation-based System Designs for Deep Offshore Wind Farms Including Power to Gas Technologies. *Appl. Energy* **2022**, *310*, 118540.
4. Zhao, J.; Xiong, Z.; Zhao, Y.; Chen, X.; Zhang, J. Two-dimensional Heterostructures for Photocatalytic CO_2 Reduction. *Environ. Res.* **2023**, *216*, 114699.
5. Mubashir, M.; Ali, M.; Bibi, Z.; Younis, M.; Muzamil, M. Efficient Hydrogen Storage in $LiMgF_3$: A First Principle Study. *Int. J. Hydrogen Energy* **2024**, *50*, 774–786.
6. Niaz, S.; Manzoor, T.; Pandith, A. H. Hydrogen Storage: Materials, Methods and Perspectives. *Renew. Sustain. Energy Rev.* **2015**, *50*, 457–469.
7. Ali, M.; Bibi, Z.; Younis, M.; Mubashir, M.; Iqbal, M.; Usman Ali, M.; Asif Iqbal, M. An Accurate Prediction of Electronic Structure, Mechanical Stability and Optical Response of $BaCuF_3$ Fluoroperovskite for Solar Cell Application. *Solar Energy* **2024**, *267*, 112199.
8. Ahluwalia, R. K.; Wang, X.; Rousseau, A.; Kumar, R. Fuel Economy of Hydrogen Fuel Cell Vehicles. *J. Power Sources* **2004**, *130* (1–2), 192–201.
9. Bououdina, M.; Grant, D.; Walker, G. J. I. J. o. H. E. Review on Hydrogen Absorbing Materials – Structure, Microstructure, and Thermodynamic Properties. *Int. J. Hydrogen Energy* **2006**, *31* (2), 177–182.
10. Bockris, J. O. M. A Hydrogen Economy. *Science* **1972**, *176* (4041), 1323.
11. Schlapbach, L.; Züttel, A. J. n. Hydrogen-storage Materials for Mobile Applications. *Nature* **2001**, *414* (6861), 353–358.
12. Wang, Q.; Zhang, M.; Fan, L.; Tao, Z. Balance the Conductivity and Enhance Chemical Stability of $BaCe_{0.3}Fe_{0.7}O_{3-\delta}$ by Tuning A-Site Cation Deficiency. *Ceram. Int.* **2024**, *50* (9), 14631–14636.
13. Elam, C. C.; Padro, C. E.; Sandrock, G.; Luzzi, A.; Lindblad, P.; Hagen, E. F. Realizing the Hydrogen Future: The International Energy Agency's Efforts to Advance Hydrogen Energy Technologies. *Int. J. Hydrogen Energy* **2003**, *28* (6), 601–607.
14. Edwards, P. P.; Kuznetsov, V.; David, W.; Brandon, N. Hydrogen and Fuel Cells: Towards a Sustainable Energy Future. *Energy Policy* **2008**, *36* (12), 4356–4362.
15. Bouhadda, Y.; Fenineche, N.; Boudouma, Y. J. P. B. C. M. Hydrogen Storage: Lattice Dynamics of Orthorhombic $NaMgH_3$. *Phys. B Condens. Matter* **2011**, *406* (4), 1000–1003.
16. Pan, Y. J. I. J. o. H. E. Theoretical Discovery of High Capacity Hydrogen Storage Metal Tetrahydrides. *Int. J. Hydrogen Energy* **2019**, *44* (33), 18153–18158.
17. Netskina, O. V.; Pochtar, A. A.; Komova, O. V.; Simagina, V. I. Solid-state $NaBH_4$ Composites as Hydrogen Generation Material: Effect of Thermal Treatment of a Catalyst Precursor on the Hydrogen Generation Rate. *Catalysts* **2020**, *10* (2), 201.
18. Sedev, R.; Akhondzadeh, H.; Ali, M.; Keshavarz, A.; Iglauer, S. Contact Angles of a Brine on a Bituminous Coal in Compressed Hydrogen. *GRL* **2022**, *49* (8), https://doi.org/10.1029/2022gl098261.
19. Zhang, Y.; Bhattacharjee, G.; Kumar, R.; Linga, P. Solidified Hydrogen Storage (Solid-HyStore) via Clathrate Hydrates. *Chem. Eng. J.* **2022**, *431*, 133702.
20. Armaroli, N.; Balzani, V. The Hydrogen Issue. *ChemSusChem* **2010**, *4* (1), 21–36.
21. Rand, D. A. J.; Dell, R. M. Hydrogen Energy: Challenges and Prospects. *RSC* **2007**.
22. Olah, G. *Beyond Oil and Gas: The Methanol Economy*; Wiley VCH: Los Angeles, 2006.
23. IEA, IRENA and UN Climate Change High-Level Champions. In *Breakthrough Agenda Report 2023. Paris, France: IEA (International Energy Agency)*; IEA: Paris, 2024.
24. Eberle, U.; Von Helmolt, R. J. E.; Science, E. Sustainable Transportation Based on Electric Vehicle Concepts: A Brief Overview. *Energy Environ. Sci.* **2010**, *3* (6), 689–699.
25. Libowitz, G. G. *Solid-state Chemistry of Binary Metal Hydrides*; W.A. Benjamin, 1965.
26. Reilly, J. J. G. D. S. *Sci. Am.* **1980**, *242* (98).
27. Skiskiewicz, T. *Phys. Status Solidi* **1972**, *A* (11 K123).
28. Zhou, L. J. R.; Reviews, S. E. Progress and Problems in Hydrogen Storage Methods. *Renew. Sustain. Energy Rev.* **2005**, *9* (4), 395–408.
29. Fakioğlu, E.; Yürüm, Y.; Veziroğlu, T. N. J. I. j. o. h. e. A Review of Hydrogen Storage Systems Based on Boron and its Compounds. *Int. J. Hydrogen Energy* **2004**, *29* (13), 1371–1376.
30. Sherif, S. A.; Barbir, F.; Veziroglu, T. J. S. e. Wind Energy and the Hydrogen Economy – Review of the Technology. *Solar Energy* **2005**, *78* (5), 647–660.
31. Jain, I.; Jain, P.; Jain, A. Novel Hydrogen Storage Materials: A Review of Lightweight Complex Hydrides. *J. Alloys Compd.* **2010**, *503* (2), 303–339.
32. Schlapbach, L.; Züttel, A. Hydrogen-storage Materials for Mobile Applications. *Nature* **2001**, *414* (6861), 353–358.
33. Ramachandran, R.; Menon, R. K. J. I. j. o. h. e. An Overview of Industrial Uses of Hydrogen. *Int. J. Hydrogen Energy* **1998**, *23* (7), 593–598.
34. Sui, Y.; Yuan, Z.; Zhou, D.; Zhai, T.; Li, X.; Feng, D.; Li, Y.; Zhang, Y. Recent Progress of Nanotechnology in Enhancing Hydrogen Storage Performance of Magnesium-Based Materials: A Review. *Int. J. Hydrogen Energy* **2022**, *47* (71), 30546–30566.
35. Li, S.; Yang, L.; Zhu, Y.; Liu, Y.; Zhang, J.; Li, L. Mechanism of Improving Hydrogenation of Mg by In-Situ Formation of Al* in Hydriding Combustion Synthesis. *J. Alloys Compd.* **2022**, *911*, 164969.
36. Qin, H.; Li, H.; Fu, Q.; Yu, R.; Zhao, Y.; Kang, Z.; Chen, X.; Wang, M. Geometric Improvement of Hydrolysis Reactor Structure to Enhance the Sustainable Production of Hydrogen from MgH_2. *Int. J. Hydrogen Energy* **2022**, *47* (77), 32990–32999.
37. Osman, A. I.; Nasr, M.; Eltaweil, A. S.; Hosny, M.; Farghali, M.; Al-Fatesh, A. S.; Rooney, D. W.; Abd El-Monaem, E. M. Advances in Hydrogen Storage Materials: Harnessing Innovative Technology, from Machine Learning to Computational Chemistry, for Energy Storage Solutions. *Int. J. Hydrogen Energy* **2024**, https://doi.org/10.1016/j.ijhydene.2024.03.223.
38. Cheng, F.; Tao, Z.; Liang, J.; Chen, J. Efficient Hydrogen Storage with the Combination of Lightweight Mg/MgH_2 and Nanostructures. *Chem. Commun.* **2012**, *48* (59), 7334–7343.
39. Wagemans, R. W.; van Lenthe, J. H.; de Jongh, P. E.; van Dillen, A. J.; de Jong, K. P. Hydrogen Storage in Magnesium Clusters: Quantum Chemical Study. *J. Am. Chem. Soc.* **2005**, *127* (47), 16675–16680.
40. Aguey-Zinsou, K.-F.; Ares-Fernández, J.-R. J. C. o. M. Synthesis of Colloidal Magnesium: A Near Room Temperature Store for Hydrogen. *Chem. Mater.* **2008**, *20* (2), 376–378.
41. Zhang, X.; Yongfeng, L.; Zhuanghe, R.; Xuelian, Z.; Jianjiang, H.; Zhenguo, H.; Yunhao, L.; Mingxia, G.; Hongge, P. Realizing 6.7 wt% Reversible Storage of Hydrogen at Ambient Temperature with Non-confined Ultrafine Magnesium Hydrides. *Energy Environ. Sci.* **2021**, *14* (4), 2302–2313.
42. Wan, H.; Yang, X.; Zhou, S.; Ran, L.; Lu, Y.; Chen, Y.; Wang, J.; Pan, F. Enhancing Hydrogen Storage Properties of MgH_2 Using FeCoNiCrMn High Entropy Alloy Catalysts. *J. Mater. Sci. Technol.* **2023**, *149*, 88–98.

43. Wan, H.; Fang, D.; Zhou, S.; Yang, X.; Dai, Y.; Ran, L.; Chen, Y.; Pan, F. Enhanced Dehydrogenation Properties and Mechanism Analysis of MgH_2 Solid Solution Containing Fe Nano-Catalyst. *Int. J. Hydrogen Energy* **2023**, *48* (87), 34180–34191.
44. Zeng, L.; Qing, P.; Cai, F.; Huang, X.; Liu, H.; Lan, Z.; Guo, J. Enhanced Hydrogen Storage Properties of MgH_2 Using a Ni and TiO_2 Co-doped Reduced Graphene Oxide Nanocomposite as a Catalyst. *Front. Chem.* **2020**, *8*, https://doi.org/10.3389/fchem.2020.00207.
45. Ebrahimi, A.; Esfahani, H.; Imantalab, O.; Fattah-Alhosseini, A. Biological, Antibacterial Activities and Electrochemical Behavior of Borided Commercially Pure Titanium in BSA-Containing PBS. *Trans. Nonferrous Met. Soc. China* **2020**, *30* (4), 944–957.
46. Salt, E. H. U. M. Special Issue for Attendees at Anomalous Nuclear Effects in Deuterium/Solid Systems Conference. *Fusion Technol.* **1990**.
47. Kubas, G. J. *Metal dihydrogen and s-bond complexes: structure, theory, and reactivity*; Springer Science & Business Media: New York, US, 2001.
48. Fray, D. J. I. M. R. Novel Methods for the Production of Titanium. *Int. Mater. Rev.* **2008**, *53* (6), 317–325.
49. Xia, Y.; Lefler, H. D.; Fang, Z. Z.; Zhang, Y.; Sun, P. Energy Consumption of the Kroll and HAMR Processes for Titanium Production. In *Extractive Metallurgy of Titanium*; Elsevier: Amsterdam, 2020; pp 389–410.
50. Ardani, M. R.; Hamid, S. A. R. S. A.; Mohamed, A. R. J. M. L. Synthesis of TiH_2 Powder from Ilmenite Using MgH_2 under H_2 Atmosphere. *Mater. Lett.* **2021**, *298*, 129997.
51. Leipunsky, I.; Zhigach, A.; Kuskov, M.; Berezkina, N.; Afanasenkova, E.; Kudrov, B.; Lopez, G.; Vorobjeva, G.; Naumkin, A. Synthesis of TiH_2 Nanopowder via the Guen-Miller Flow-Levitation Method and Characterization. *J. Alloys Compd.* **2019**, *778*, 271–279.
52. Gawley, R. E. D.; Arnold *Calcium Hydride. Encyclopedia of Reagents for Organic Synthesis*; John Wiley & Sons, Ltd, 2001.
53. Xiao, C.-Y.; Yang, J. L.; Deng, K. M.; Bian, Z. H.; Wang, K. L. Electronic Structure and Compton Profile of CaH_2. *J. Phys.: Condens. Matter* **1994**, *6* (41), 8539.
54. Catlow, C. J. D. i. S. M. T. Computer simulation of defects in solids. *Defects in Solids: Mod. Tech.* **1986**, 269–301.
55. Dovesi, R.; Roetti, C.; Freyria-Fava, C.; Prencipe, M.; Saunders, V. On the Elastic Properties of Lithium, Sodium and Potassium Oxide. An Ab Initio Study. *Chem. Phy.* **1991**, *156* (1), 11–19.
56. Catti, M.; Pavese, A.; Dovesi, R.; Roetti, C.; Causà, M. Quantum-mechanical Hartree-Fock Self-Consistent-Field Study of the Elastic Constants and Chemical Bonding of MgF_2 (Sellaite). *Phys. Rev. B.* **1991**, *44* (8), 3509.
57. El Gridani, A.; El Mouhtadi, M. J. C. P. Electronic and Structural Properties of CaH_2: An Ab Initio Hartree–Fock Study. *Chem. Phy.* **2000**, *252* (1–2), 1–8.
58. Ma, L.; Wang, K.; Xie, Y.; Yang, X.; Wang, Y.; Zhou, M.; Liu, H.; Yu, X.; Zhao, Y.; Wang, H.; Liu, G.; Ma, Y. High-temperature Superconducting Phase in Clathrate Calcium Hydride CaH_6 up to 215 K at a Pressure of 172 GPa. *Phy. Rev. Letters* **2022**, *128* (16), 167001.
59. Wang, H.; Tse, J. S.; Tanaka, K.; Iitaka, T.; Ma, Y. Superconductive Sodalite-like Clathrate Calcium Hydride at High Pressures. *PNAS* **2012**, *109* (17), 6463–6466.
60. Sun, Y.; Zhong, X.; Liu, H.; Ma, Y. Clathrate Metal Superhydrides under High-Pressure Conditions: Enroute to Room-Temperature Superconductivity. *Natl. Sci. Rev.* **2024**, *11* (7), https://doi.org/10.1093/nsr/nwad270.
61. An, D.; Duan, D.; Zhang, Z.; Jiang, Q.; Ma, T.; Huo, Z.; Song, H.; Cui, T. Type-I Clathrate Calcium Hydride and its Hydrogen-Vacancy Structures at High Pressure. *Phys. Rev. B.* **2024**, *110* (5), 054505.
62. Ma, L.; Kui, W.; Yu, X.; Xin, Y.; Yingying, W.; Mi, Z.; Hanyu, L.; Xiaohui, Y.; Yongsheng, Z.; Hongbo, W.; Guangtao, L.; Yanming, M. High-Tc Superconductivity in Clathrate Calcium Hydride CaH_6. *arXiv preprint arXiv* **2021**.
63. Orgaz, E.; Membrillo, A.; Castañeda, R.; Aburto, A. Electronic Structure of Ternary Hydrides Based on Light Elements. *J. Alloys Compd.* **2005**, *404*, 176–180.
64. Paskevicius, M.; Jepsen, L. H.; Schouwink, P.; Černý, R.; Ravnsbæk, D. B.; Filinchuk, Y.; Dornheim, M.; Besenbacher, F.; Jensen, T. R. Metal Borohydrides and Derivatives–Synthesis, Structure and Properties. *Chem. Soc. Rev.* **2017**, *46* (5), 1565–1634.
65. Fedneva, E.; Alpatova, V.; Mikheeva, V. J. R. J. I. C. $LiBH_4$ Complex Hydride Materials. *Russ. J. Inorg. Chem.* **1964**, *9*, 826–827.
66. Schlesinger, H.; Brown, H. C. J. J. o. t. A. C. S. Metallo Borohydrides. III. Lithium Borohydride. *J. Am. Chem. Soc.* **1940**, *62* (12), 3429–3435.
67. Hou, J.; Huang, S.; Chen, J.; Yang, Y.; Tao, P.; Ouyang, L.; Wang, H.; Yang, X. Altering the Chemical State of Boron Towards the Facile Synthesis of $LiBH_4$ via Hydrogenating Lithium Compound-Metal Boride Mixture. *Renew. Energy* **2019**, *134*, 235–240.
68. Ouyang, L.; Chen, W.; Liu, J.; Felderhoff, M.; Wang, H.; Zhu, M. Enhancing the Regeneration Process of Consumed $NaBH_4$ for Hydrogen Storage. *Adv. Energy Mater.* **2017**, *7* (19), 1700299.
69. Zhu, Y.; Ouyang, L.; Zhong, H.; Liu, J.; Wang, H.; Shao, H.; Huang, Z.; Zhu, M. Closing the Loop for Hydrogen Storage: Facile Regeneration of $NaBH_4$ from its Hydrolytic Product. *Angew. Chem.* **2020**, *132* (22), 8701–8707.
70. Yang, Y.; Wu, X.; Liu, C.; Huang, S. Density Functional Theory Study of Neutral and Singly-Charged ($NaBH_4$) N (N= 1–6) Nanoclusters. *Chem. Phy.* **2014**, *443*, 45–52.
71. Chen, K.; Ouyang, L.; Zhong, H.; Liu, J.; Wang, H.; Shao, H.; Zhang, Y.; Zhu, M. Converting H+ from Coordinated Water into H− Enables Super Facile Synthesis of $LiBH_4$. *Green Chem.* **2019**, *21* (16), 4380–4387.
72. Soulié, J.-P.; Renaudin, G.; Černý, R.; Yvon, K. Lithium Boro-Hydride $LiBH_4$: I. Crystal Structure. *J. Alloys Compd.* **2002**, *346* (1–2), 200–205.
73. Züttel, A.; Wenger, P.; Rentsch, S.; Sudan, P.; Mauron, P.; Emmenegger, C. $LiBH_4$ a New Hydrogen Storage Material. *J. Power Sources* **2003**, *118* (1–2), 1–7.
74. Züttel, A.; Borgschulte, A.; Orimo, S.-I. J. S. M. Tetrahydroborates as New Hydrogen Storage Materials. *Scr. Mater.* **2007**, *56* (10), 823–828.
75. Nakamori, Y.; Orimo, S. Borohydrides as Hydrogen Storage Materials. In *Solid-state hydrogen storage*; Elsevier: Amsterdam, 2008; pp 420–449.
76. Barkhordarian, G.; Klassen, T.; Dornheim, M.; Bormann, R. Unexpected Kinetic Effect of MgB_2 in Reactive Hydride Composites Containing Complex Borohydrides. *J. Alloys Compd.* **2007**, *440* (1–2), L18–L21.
77. Rönnebro, E.; Majzoub, E. H. J. T. J. o. P. C. B. Calcium Borohydride for Hydrogen Storage: Catalysis and Reversibility. *J. Phys. Chem.* **2007**, *111* (42), 12045–12047.
78. Matsunaga, T.; Buchter, F.; Mauron, P.; Bielman, M.; Nakamori, Y.; Orimo, S.; Ohba, N.; Miwa, K.; Towata, S.; Züttel, A. Hydrogen Storage Properties of Mg $[BH_4]_2$. *J. Alloys Compd.* **2008**, *459* (1–2), 583–588.
79. Huang, Y.; Cheng, Y.; Zhang, J. A Review of High Density Solid Hydrogen Storage Materials by Pyrolysis for Promising Mobile Applications. *Ind. Eng. Chem. Res.* **2021**, *60* (7), 2737–2771.
80. Orimo, S.-I.; Nakamori, Y.; Kitahara, G.; Miwa, K.; Ohba, N.; Towata, S. I.; Züttel, A. Dehydriding and rehydriding reactions of $LiBH_4$. *J. Alloys Compd.* **2005**, *404*, 427–430.
81. Luo, Y.; Sun, L.; Xu, F.; Liu, Z. Improved Hydrogen Storage of $LiBH_4$ and NH_3BH_3 by Catalysts. *J. Mater. Chem.* **2018**, *6* (17), 7293–7309.

82. Mauron, P.; Buchter, F.; Friedrichs, O.; Remhof, A.; Bielmann, M.; Zwicky, C. N.; Züttel, A. Stability and Reversibility of $LiBH_4$. *J. Phys. Chem.* **2008**, *112* (3), 906–910.
83. Urgnani, J.; Torres, F.; Palumbo, M.; Baricco, M. Hydrogen Release from Solid State $NaBH_4$. *Int. J. Hydrogen Energy* **2008**, *33* (12), 3111–3115.
84. Muir, S. S.; Yao, X. J. I. J. o. H. E. Progress in Sodium Borohydride as a Hydrogen Storage Material: Development of Hydrolysis Catalysts and Reaction Systems. *Int. J. Hydrogen Energy* **2011**, *36* (10), 5983–5997.
85. Guo, Y.; Jia, J.; Wang, X. H.; Ren, Y.; Wu, H. Prediction of Thermodynamically Reversible Hydrogen Storage Reactions in the KBH_4/M (M= Li, Na, Ca)(BH_4) N (N= 1, 2) System from First-Principles Calculation. *Chem. Phy.* **2013**, *418*, 22–27.
86. Clémençon, D.; Davoisne, C.; Chotard, J. N.; Janot, R. Enhancement of the Hydrogen Release of Mg $(BH_4)_2$ by Concomitant Effects of Nano-Confinement and Catalysis. *Int. J. Hydrogen Energy* **2019**, *44* (8), 4253–4262.
87. Chong, M.; Matsuo, M.; Orimo, S. i.; Autrey, T.; Jensen, C. M. Selective Reversible Hydrogenation of Mg $(B_3H_8)_2/MgH_2$ to Mg $(BH_4)_2$: Pathway to Reversible Borane-Based Hydrogen Storage? *Inorg. Chem.* **2015**, *54* (8), 4120–4125.
88. Jena, P. J. T. J. o. P. C. L. Materials for Hydrogen Storage: Past, Present, and Future. *J. Phys. Chem. Lett.* **2011**, *2* (3), 206–211.
89. Kim, C.; Hwang, S. J.; Bowman, R. C., Jr.; Reiter, J. W.; Zan, J. A.; Kulleck, J. G.; Kabbour, H.; Majzoub, E. H.; Ozolins, V. LiSc $(BH_4)_4$ as a Hydrogen Storage Material: Multinuclear High-Resolution Solid-State NMR and First-Principles Density Functional Theory Studies. *J. Phys. Chem.* **2009**, *113* (22), 9956–9968.
90. Li, H.-W.; Orimo, S.; Nakamori, Y.; Miwa, K.; Ohba, N.; Towata, S.; Züttel, A. Materials Designing of Metal Borohydrides: Viewpoints from Thermodynamical Stabilities. *J. Alloys Compd.* **2007**, *446*, 315–318.
91. Nakamori, Y.; Li, H. W.; Kikuchi, K.; Aoki, M.; Miwa, K.; Towata, S.; Orimo, S. Thermodynamical Stabilities of Metal-Borohydrides. *J. Alloys Compd.* **2007**, *446*, 296–300.
92. Hwang, S.; Bowman, R.; Reiter, J. J. J. P. C. C.; Soloveichik, G. L.; Zhao, J.-C.; Kabbour, H.; Ahn, C. C. N. M. Confirmation for Formation of $[B_{12}H_{12}]^{2-}$ Complexes During Hydrogen Desorption from Metal Borohydrides. *J. Phys. Chem.* **2008**, *112* (9), 3164–3169.
93. Jena, P. Materials Issues in a Hydrogen Economy. In *Proceedings of the International Symposium, Richmond, Virginia, USA, 12–15 November 2007*; World Scientific, 2009.
94. Hagemann, H.; Longhini, M.; Kaminski, J. W.; Wesolowski, T. A.; Černý, R.; Penin, N.; Sørby, M. H.; Hauback, B. C.; Severa, G.; Jensen, C. M. LiSc $(BH_4)_4$: A Novel Salt of Li+ and Discrete Sc $(BH_4)_4^-$ Complex Anions. *J. Phys. Chem.* **2008**, *112* (33), 7551–7555.
95. Purewal, J.; Hwang, S. J.; Bowman, R. C., Jr.; Rönnebro, E.; Fultz, B.; Ahn, C. Hydrogen Sorption Behavior of the ScH_2–$LiBH_4$ System: Experimental Assesment of Chemical Destabilization Effects. *J. Phys. Chem.* **2008**, *112* (22), 8481–8485.
96. Ley, M. B.; Boulineau, S.; Janot, R.; Filinchuk, Y.; Jensen, T. R. New Li Ion Conductors and Solid State Hydrogen Storage Materials: LiM $(BH_4)_3Cl$, M= La, Gd. *J. Phys. Chem.* **2012**, *116* (40), 21267–21276.
97. Nguyen, J.; Fleutot, B.; Janot, R. J. S. S. I. Investigation of the Stability of Metal Borohydrides-Based Compounds LiM $(BH_4)_3Cl$ (M= La, Ce, Gd) as Solid Electrolytes for Li-S Batteries. *Solid State Ion.* **2018**, *315*, 26–32.
98. Ley, M. B.; Ravnsbæk, D. B.; Filinchuk, Y.; Lee, Y. S.; Janot, R.; Cho, Y. W.; Skibsted, J.; Jensen, T. R. LiCe $(BH_4)_3Cl$, a New Lithium-Ion Conductor and Hydrogen Storage Material with Isolated Tetranuclear Anionic Clusters. *Chem. Mater.* **2012**, *24* (9), 1654–1663.
99. Mak, T. C.; Mok, F.-C. J. J. o. C.; Structure, M. Inorganic Cages Related to Cubane and Adamantane. *J. Mol. Struct.* **1978**, *8* (4), 183–191.
100. Borislav, B.; Manfred, S. Ti-Doped Alkali Metal Aluminium Hydrides as Potential Novel Reversible Hydrogen Storage Materials. *J. Alloys Compd.* **1997**, *253*, 1–9.
101. Chen, P.; Xiong, Z.; Luo, J.; Lin, J.; Tan, K. L. Interaction of Hydrogen with Metal Nitrides and Imides. *Nature* **2002**, *420* (6913), 302–304.
102. Züttel, A. Materials for Hydrogen Storage. *Mater. Today* **2003**.
103. Finholt, A. E. G. C. B.; Barbaras, G. K.; Urry, G.; Wartik, T.; Schlesinger, H. I. *J. Inorg. Nucl. Chem.* **1955**, *69*, 317.
104. Niaz, S.; Manzoor, T.; Pandith, A. H. Hydrogen Storage: Materials, Methods and Perspectives. *Renew. Sustain. Energy Rev.* **2015**, *50*, 457–469.
105. Global, I. Energy & CO_2 Status Report. *IEA* **2018**.
106. Ikeda, K.; Kogure, Y.; Nakamori, Y.; Orimo, S. Formation Region and Hydrogen Storage Abilities of Perovskite-type Hydrides. *Prog. Solid State Chem.* **2007**, *35* (2–4), 329–337.
107. Pottmaier, D.; Pinatel, E. R.; Vitillo, J. G.; Garroni, S.; Orlova, M.; Baró, M. D.; Vaughan, G. B. M.; Fichtner, M.; Lohstroh, W.; Baricco, M. Structure and Thermodynamic Properties of the $NaMgH_3$ Perovskite: A Comprehensive Study. *Chem. Mater.* **2011**, *23* (9), 2317–2326.
108. Reshak, A. J. I. J. o. H. E. $NaMgH_3$ a Perovskite-type Hydride as Advanced Hydrogen Storage Systems: Electronic Structure Features. *Int. J. Hydrogen Energy* **2015**, *40* (46), 16383–16390.
109. Al, S.; Cavdar, N.; Arikan, N. Computational Evaluation of Comprehensive Properties of MgX_3H_8 (X= Sc, Ti and Zr) as Effective Solid State Hydrogen Storage Materials. *J. Energy Storage* **2024**, *80*, 110402.
110. Al, S.; Yortanlı, M.; Mete, E. Lithium Metal Hydrides (Li_2CaH_4 and Li_2SrH_4) for Hydrogen Storage; Mechanical, Electronic and Optical Properties. *Int. J. Hydrogen Energy* **2020**, *45* (38), 18782–18788.
111. Broom, D. P. *Hydrogen Storage Materials: The Characterisation of Their Storage Properties*; Springer: Berlin, Vol. 1, 2011.
112. Al, S.; Cavdar, N.; Arikan, N. J. J. o. E. S. Computational Evaluation of Comprehensive Properties of MgX_3H_8 (X= Sc, Ti and Zr) as Effective Solid State Hydrogen Storage Materials. *J. Energy Storage* **2024**, *80*, 110402.
113. Al, S.; Kurkcu, C.; Yamcicier, C. Structural Evolution, Mechanical, Electronic and Vibrational Properties of High Capacity Hydrogen Storage TiH_4. *Int. J. Hydrogen Energy* **2020**, *45* (55), 30783–30791.
114. Al, S. Theoretical Investigations of Elastic and Thermodynamic Properties of $LiXH_4$ Compounds for Hydrogen Storage. *Int. J. Hydrogen Energy* **2019**, *44* (3), 1727–1734.
115. Pan, Y.; Chen, S. Exploring the Novel Structure, Transportable Capacity and Thermodynamic Properties of TiH_2 Hydrogen Storage Material. *Int. J. Energy Res.* **2020**, *44* (6), 4997–5007.
116. Xu, N.; Chen, Y.; Chen, S.; Li, S.; Zhang, W. First-principles Investigation for the Hydrogen Storage Properties of $XTiH_3$ (X= K, Rb, Cs) Perovskite Type Hydrides. *Int. J. Hydrogen Energy* **2024**, *50*, 114–122.
117. Gencer, A.; Surucu, G.; Al, S. J. I. J. O. H. E. $MgTiO_3Hx$ and $CaTiO_3Hx$ Perovskite Compounds for Hydrogen Storage Applications. *Int. J. Hydrogen Energy* **2019**, *44* (23), 11930–11938.
118. Gencer, A.; Surucu, G. J. I. J. O. H. E. Properties of $BaYO_3$ Perovskite and Hydrogen Storage Properties of $BaYO_3Hx$. *Int. J. Hydrogen Energy* **2020**, *45* (17), 10507–10515.
119. Broom, D. P. Hydrogen sorption properties of materials. *HSM* **2011**, 61–115.
120. Rehmat, B.; Rafiq, M.; Javed, Y.; Irshad, Z.; Ahmed, N.; Mirza, S. Elastic Properties of Perovskite-type Hydrides $LiBeH_3$ and $NaBeH_3$ for Hydrogen Storage. *Int. J. Hydrogen Energy* **2017**, *42* (15), 10038–10046.

121. Bell, N. A.; Coates, G. E. Lithium and Sodium Beryllium Hydrides. *J. Chem. Soc., A: Inorganic, Physical, Theoretical* **1968**, 628–631.
122. Tamássy-Lentei, I.; Szaniszló, J. J. A. P. H. Ab Initio Theoretical Study of the Structures and Stabilities of the $LiBeH_3$, Li_2BeH_4 and $LiBe_2H_5$ Molecules. *Acta Phys. Hung.* **1989**, *65* (2), 265–270.
123. Gupta, M.; Percheron-Guegan, A. J. J. o. P. F. M. P. Electronic Structure and Electron-Phonon Coupling in $LiBeH_3$. *J. Phys. F: Met. Phys.* **1987**, *17* (9), L201.
124. Seel, M.; Kunz, A.; Hill, S. J. P. R. B. Electronic Structure of Lithium Beryllium Hydride. *Phys. Rev. B.* **1989**, *39* (11), 7949.
125. Ming, Li. Band structure study on LiBeH3− y. *Int. J. Quantum Chem.* **1998**, *68* (6), 415–419.
126. Xiao-Jiao, S.; Zhi, H.; Yan-Ming, M.; Tian, C.; Bing-Bing, L.; Guang-Tian, Z. Electronic Structure and Optical Properties of $LiXH_3$ and $XLiH_3$ (X= Be, B or C). *Chin. Phys. B.* **2008**, *17* (6), 2222.
127. Hu, C.-H.; Oganov, A. R.; Wang, Y. M.; Zhou, H. Y.; Lyakhov, A.; Hafner, J. Crystal Structure Prediction of $LiBeH_3$ Using Ab Initio Total-Energy Calculations and Evolutionary Simulations. *J. Chem. Phys.* **2008**, *129* (23), https://doi.org/10.1063/1.3021079.
128. Hu, C.-H.; Oganov, A. R.; Lyakhov, A. O.; Zhou, H. Y.; Hafner, J. Insulating States of $LiBeH_3$ under Extreme Compression. *PRB—CMMP* **2009**, *79* (13), 134116.
129. y Blancá, E. L. P. First Principle Predictions of New Crystal Structures for Hydrogen Reservoirs. *Int. J. Hydrogen Energy* **2016**, *41* (13), 5682–5687.
130. Boettger, J. J. I. J. O. Q. C. Theoretical Properties of a 3-layer Film of $LiBeH_3$. *Int. J. Quantum Chem.* **1991**, *40* (S25), 629–639.
131. Vajeeston, P.; Ravindran, P.; Fjellvåg, H. A New Series of High Hydrogen Content Hydrogen-Storage Materials – A Theoretical Prediction. *J. Alloys Compd.* **2007**, *446*, 44–47.
132. Vajeeston, P.; Ravindran, P.; Fjellvåg, H. J. I. c. Structural Phase Stability Studies on $MBeH_3$ (M= Li, Na, K, Rb, Cs) from Density Functional Calculations. *Inorg. Chem.* **2008**, *47* (2), 508–514.
133. Karazhanov, S. Z.; Ravindran, P.; Vajeeston, P.; Ulyashin, A.; Finstad, T. G.; Fjellvåg, H. Phase Stability, Electronic Structure, and Optical Properties of Indium Oxide Polytypes. *PRB—CMMP* **2007**, *76* (7), 075129.
134. Sanchez-Castro, M. E.; Sanchez-Vazquez, M. J. J. o. M. S. Electronic and Structural Study of $[BeH_3]^-$ Ligands Coordinated to Alkali-Metals. *J. Mol. Struct.* **2010**, *969* (1–3), 204–207.
135. Rafique, A.; Usman, M.; Rehman, J. U.; Nazeer, A.; Ullah, H.; Hussain, A. Investigation of Structural, Electronic, Mechanical, Optical and Hydrogen Storage Properties of Cobalt-Based Hydride-Perovskites $XCoH_3$ (X= in, Mn, Sr, Sn, Cd) for Hydrogen Storage Application. *J. Phys. Chem. Solids* **2023**, *181*, 111559.
136. Usman, M.; Rehman, J. u.; Tahir, M. B.; Hussain, A.; Alrobei, H.; Alzaid, M.; Dahshan, A. First-principles Calculations to Investigate Structural, Electronics, Optical, and Mechanical Properties of Bi-based Novel Fluoroperovskites $TBiF_3$ (T= Hg, Xe) for Optoelectronic Applications. *Mat. Sci. Semicon. Proc.* **2023**, *160*, 107399.
137. Xu, N.; Chen, Y.; Chen, S.; Zhang, W.; Li, S.; Song, R.; Zhang, J. First-principles Investigations for the Hydrogen Storage Properties of XVH_3 (X¼Na, K, Rb, Cs) Perovskite Type Hydrides. *J. Mater. Res. Technol.* **2023**, *2* (6), 4825.
138. Murnaghan, F. D. J. P. O. T. N. A. O. S. The Compressibility of Media under Extreme Pressures. *Proc. Natl. Acad. Sci.* **1944**, *30* (9), 244–247.
139. Candan, A.; Kurban, M. J. S. S. C. Electronic Structure, Elastic and Phonon Properties of Perovskite-type Hydrides $MgXH_3$ (X= Fe, Co) for Hydrogen Storage. *Solid State Commun.* **2018**, *281*, 38–43.
140. Siddique, A.; Khalil, A.; Almutairi, B. S.; Tahir, M. B.; Ahsan, T.; Hannan, A.; Alzaid, M. Structural, Electronic, Mechanical and Dynamical Stability Properties of $LiAH_3$ (A= Sc, Ti & V) Perovskite-type Hydrides: A First Principle Study. *Chem. Phy.* **2023**, *568*, 111851.
141. Siddique, A.; Khalil, A.; Almutairi, B. S.; Tahir, M. B.; Sagir, M.; Ullah, Z.; Hannan, A.; Ali, H. E.; Alrobei, H.; Alzaid, M. Structures and Hydrogen Storage Properties of $AeVH_3$ (Ae= Be, Mg, Ca, Sr) Perovskite Hydrides by DFT Calculations. *Int. J. Hydrogen Energy* **2023**, *48* (63), 24401–24411.
142. Garara, M.; Benzidi, H.; Abdellaoui, M.; Lakhal, M.; El kenz, A.; Benyoussef, A.; Mounkachi, O.; Loulidi, M. Hydrogen Storage Properties of Perovskite-type $MgCoH_3$ under Strain Effect. *Mater. Chem. Phys.* **2020**, *254*, 123417.
143. Togo, A.; Tanaka, I. J. S. M. First Principles Phonon Calculations in Materials Science. *Scr. Mater.* **2015**, *108*, 1–5.
144. Vegge, T.; Hedegaard-Jensen, L. S.; Bonde, J.; Munter, T. R.; Noerskov, J. K. Trends in Hydride Formation Energies for Magnesium-3d Transition Metal Alloys. *J. Alloys Compd.* **2005**, *386* (1–2), 1–7.
145. Abdellaoui, M.; Lakhal, M.; Benzidi, H.; Mounkachi, O.; Benyoussef, A.; El Kenz, A.; Loulidi, M. The Hydrogen Storage Properties of Mg-Intermetallic-Hydrides by Ab Initio Calculations and Kinetic Monte Carlo Simulations. *Int. J. Hydrogen Energy* **2020**, *45* (19), 11158–11166.